Triplet states in derivatives of polyfluorene and polyspirobifluorene

Simon King

Triplet States in Derivatives of Polyfluorene and Polyspirobifluorene

Simon King

Submitted for the Degree of MSc, 2005

Studies of the triplet excitons in polyspirobifluorene have been carried out principally the techniques of photoinduced absorption and gated emission. Specifically the nature of the origin of the delayed emission has been investigated. In dilute solutions delayed fluorescence is attributed to intrachain triplet-triplet annihilation, whereas in thin films the delayed fluorescence is shown to originate from both inter and intra chain annihilation processes. In dilute solutions the use of time resolved photoinduced absorption has proven the production of triplets via intersystem crossing. In addition in dilute solutions the observation of triplet-triplet annihilation in the absence of singlet-singlet annihilation has shown that the singlet excitons are relatively immobile along the chains compared with the triplet excitons.

In addition to the triplet studies of PSBF, investigations were made into oligomers of the polyfluorene derivative Pf 2/6. Absorption and photoinduced absorption studies have shown that the triplet exciton is intrinsically confined to approximately 5 repeat units of the polymer, whereas the singlet occupies a considerably larger conjugation length of approximately 25 units. In another derivative, PFO the effect of the presence of the β-phase on the photoinduced absorption spectra has been investigated for both poor solvents and in films. Principally a shifted photoinduced absorption spectrum is observed along with the features for the amorphous polymer, in addition the low luminescence of the β-phase allows a higher transition of the triplet to be observed.

Finally we have shown that it is possible to manipulate the rate of guest host triplet back transfer between the phosphor and the polymer host in an organic phosphor doped polymer system by exploiting the short range nature of Dexter energy transfer. Derivatives of $Ir(PPY)_3$ with bulky side groups were shown to have a reduced rate of back transfer in comparison to the unsubstituted $Ir(PPY)_3$ complex.

Triplet States in Derivatives of Polyfluorene and Polyspirobifluorene

By Simon King

A thesis submitted to the Faculty of Science, The University of Durham, for the degree of Master of Science

Organic Electroactive Materials Group
Department Of Physics
University Of Durham
October 2004

Acknowledgements

Throughout the past year many people have provided support to me during my studies and although I can only name a few of them I am grateful to all those who have contributed if even in a small way to the success and enjoyment of my MSc. Most importantly my supervisor, Andy Monkman who has provided the support without which my MSc would not have been possible. Also to the entire OEM group, Helen, Ben, Fernando, Hameed, Susi, Matti, Naveed and especially Carsten who provided me with many pointers and helpful suggestions throughout the year in his own inimitable way.

I must also thank my friends and family for the support they have given me throughout the year, I am especially grateful to my parents for paying the tuition fees which allowed me to do this degree.

Finally I am very grateful to Covion Organic Semiconductor Gmbh, Professor U. Scherf at the Max-Planck-Institute for Polymer research, Dr Batsanov and Dr A. Beeby, at The Department of Chemistry, University of Durham, for providing the polymers and Complexes used in the study.

Declaration

The material in this thesis has not been submitted for examination for any other degree or part thereof, at Durham University or any other institution. The material in this thesis is the work of the author except where formally acknowledged by reference.

Table of Contents

Table of Figures

Introduction

Ever since 1990 when the first electroluminescent devices based on conjugated polymers were developed[1] by *Burroughes et al* the investigations into conjugated polymers for use in photonics have become more and more advanced. It is easy to see why, there are many possible applications from flat panel display screens to solar cells and polymer lasers[2-5]. There are many advantages that conjugated polymer devices hold over conventional inorganic LEDs and liquid crystal display systems, most of them holding economic potential. These advantages all arise from the nature of the polymers themselves, we only need to look at the way that plastics have transformed everyday life in the twentieth century to see the many advantages polymers have. One of the most promising aspects is the processability of polymers themselves, in the solution state polymers are easily handled and devices can be made by simply building up layers of polymers on a substrate through spin coating, inkjet printing, and roll to roll processing techniques[6]. Full colour displays have already been manufactured by inkjet printing onto a simple flat substrate which represent a massive leap in comparison to the complex lithographic techniques required for conventional inorganic LEDs and the expensive substrates required for other technologies. With more and more demands being made for flexible displays the amorphous nature, flexibility and relative resistance to defects of conjugated polymers makes them the ideal candidate, in situations where the lack of durability of conventional displays, such as LCDs, poses a problem.

However, as with every emerging technology there are a number of problems, two of the principal issues are with low efficiencies and colour stability. To a certain

extent these problems can be circumvented by blending polymers with other organic emitters, know as phosphorescent dyes[7], as has been demonstrated on numerous occasions, other possibilities include the use of white emitting polymer blends[8] with colour filters as well as increasing the sophistication of the polymers themselves.

This research is concerned principally with the study of the triplet states of a particular class of conjugated polymer, the polyfluorenes. Polyfluorenes are one of the latest types of conjugated polymer to be employed in PLED applications, having been developed after the original PPVs (poly-phenylenevinylenes). They are blue emitters which can easily be adapted to other colours through copolymerisation with other monomers. Research into the triplet states of these materials is essential not only as they can be responsible for one of the principal losses of efficiency in conjugated polymer devices but it is essential factor which must be considered when blending with phosphorescent dyes.

Chapter 1

Chemical bonding and Molecular orbital theory

The most simplistic theory about covalent bonding is based around the sharing of electrons. Although this may provide a convenient model when dealing with simple molecules such as methane and water it is necessary to adopt more complex ideas when dealing with larger organic systems. The commonly held theory of bonding[9] in the type of system studied here is molecular orbital theory; this envisages the atomic orbitals of the unbonded atoms mixing through overlaps to form an overall set of orbitals for the bonded molecules.

As s first step we can consider the bonding in a diatomic molecule such as H_2, the two s orbitals on the H atoms interact, merging to form a molecular orbital of lower energy than the individual s-orbitals. This molecular orbital becomes filled with the two electrons from the hydrogen atoms and the H_2 molecule is formed, this is known as a σ-bond. However, one of the fundamental considerations of molecular orbital theory is the conservation of orbitals, the two s–orbitals from the hydrogen atoms must form another orbital in addition to the σ-bonding orbital. This is of higher energy than the original orbitals and known as an antibonding orbital and is denoted by an asterisk, in the hydrogen molecule this is unfilled. In other molecules if the antibonding orbitals are filled then no bond can form.

Molecular orbital theory becomes more complicated for larger atoms and more complex molecules. Firstly the individual atomic orbitals have been established from quantum mechanical simulations and adopt a variety of shapes, as shown in figure 1.1. In a bonded system these orbitals become mixed into what are known as hybrid orbitals, the most common hybrid is that found in a saturated carbon system, i.e. one containing no double bonds, this is known as an sp^3 hybrid. The sp^3 orbital is a mixture of the s and 3 p orbitals, the p_x, the p_y and the p_z and yields a three dimensionally symmetric tetrahedral shape of the sp^3 orbital, with one lobe for each of the carbon atom's 4 valence electrons to bond through. This is shown most easily in the methane molecule in which 4 hydrogen atoms bond identically giving a bond angle of 109.5°, this type of bond is known as a σ-bond.

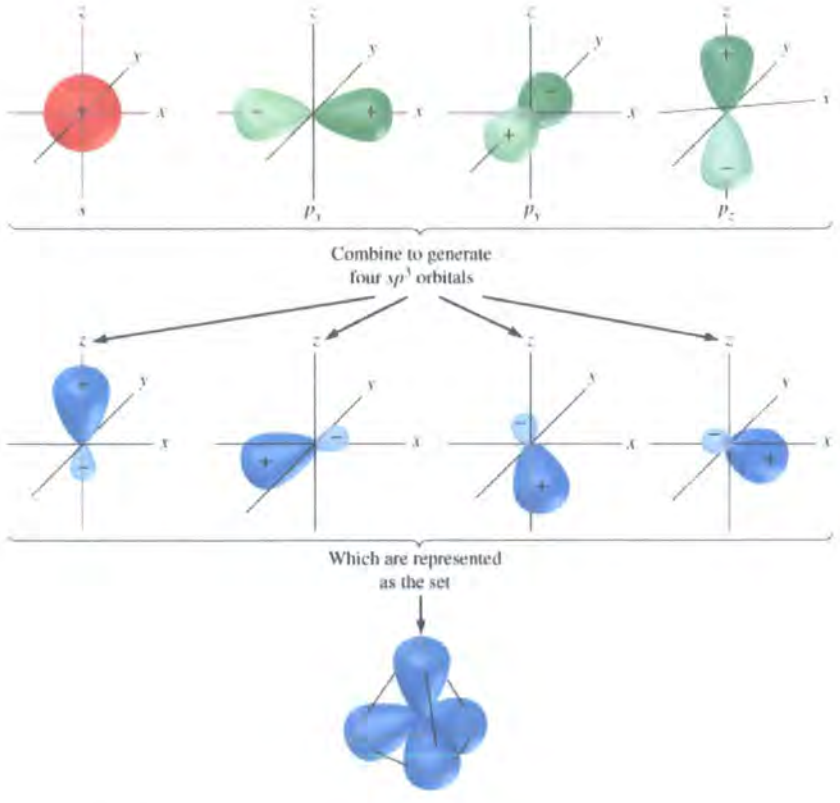

Figure 1.1 The formation of sp^3 hybrid orbitals from s and p atomic orbitals[10].

In an unsaturated carbon system, such as a conjugated polymer, the hybridization is different, only the p_x and p_y orbitals mix with the s orbital; the p_z is left unaffected. This is known as an sp^2 hybrid in which only three σ-bonds can form, this leaves one valence electron left in the p_z orbital, allowing the formation of another type of bond, the π-bond, as shown in figure 1.2; the formation of a π-bond in addition to a σ-bond between two atoms results in a double bond. It is interesting to note the orientation of the bonds with respect to the orbitals, in the σ-bond the orbital interaction is along the line of the bond, thus allowing free rotation about the axis of the bond. However, the π-bond has its interacting orbitals in a direction pointing perpendicular to the axis of the bond, the effect of this is that the bond is locked and there can be no rotation about the c – c axis as this would break the π- bond, forcing the molecule to adopt a planar structure. A further hybrid state can be formed, which is found in triply bonded molecules, whereby only one p orbital mixes with the s orbital thus allowing the formation of two π-bonds this is known as sp hybridization. It is important to think about the effect of the additional interaction on the bond itself, the stronger bonding interaction results in a shorter bond length as there is more electron density pulling the atoms together.

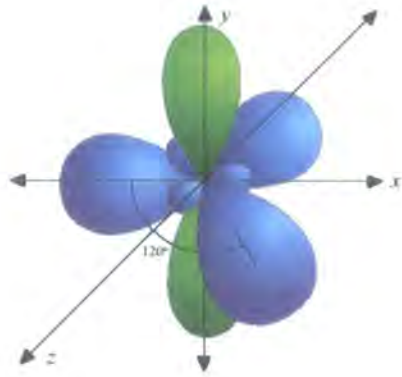

Figure 1.2 An sp^2 hybrid orbital is shown in purple and the p_y orbital remaining after hybridization is shown in green, note the planarity of the sp^2 orbital and the p_y orbital sticking vertically out of the plane of the molecule.

The construction of molecular orbitals which fill with the electrons of the atoms that take part in the bond naturally allows for the lowest energy orbitals to be filled first. As in a bonded molecule the orbitals cannot all be filled there is a level of filling which is known by the term HOMO, for highest occupied molecular orbital. Correspondingly the LUMO is the lowest unoccupied molecular orbital. In addition to this we can define a SOMO which is a singularly occupied molecular orbital, i.e. an orbital that is only filled with one electron rather than the pair found in the HOMO.

Conjugation

If we move away from a two carbon system, to something longer, such as the polymer polyacetylene which is shown in figure 1.3 we can see that the π-orbitals on the neighbouring carbons that are not π-bonded together are just as able to interact as those with a bond. This allows the electrons in the π-bonds to become delocalised along the whole chain, effectively making the whole chain one long homogenous unit.

This is only possible when the molecule contains alternating single and double bonds, this is known as a conjugated molecule. This has an important consequence on the electrical and electronic properties of the polymer. Firstly the polymer can become electrically conductive when sufficient additional electrons are added to the system through doping as the electrons are able to move freely along the polymer backbone through the π-system without interfering with the σ-bonding of the polymer, so an electric current can flow along the polymer. Although the simplistic picture is of a homogenous unit this is in fact not the case, the molecule is distorted by Jahn-Teller and Peierls distortion on the bonding. Increased interaction from the π-bond shortens the length of the double bond so that the lowest energy state is not completely symmetrical like the traditional resonance picture suggests, a dimerised state is formed. This distortion forces a band gap to develop so that the polymer is intrinsically an insulator, with doping required to form a partially filled band and allow conduction, rather than metallic, as such conjugated polymers keep a well defined HOMO and LUMO level. The effect on the electronic properties is also significant as increased conjugation acts to raise the energy of the HOMO (highest occupied molecular orbital and lower the energy of the LUMO (lowest unoccupied molecular orbital) this is important as it effectively lowers the energy of electronic transitions in the molecule.

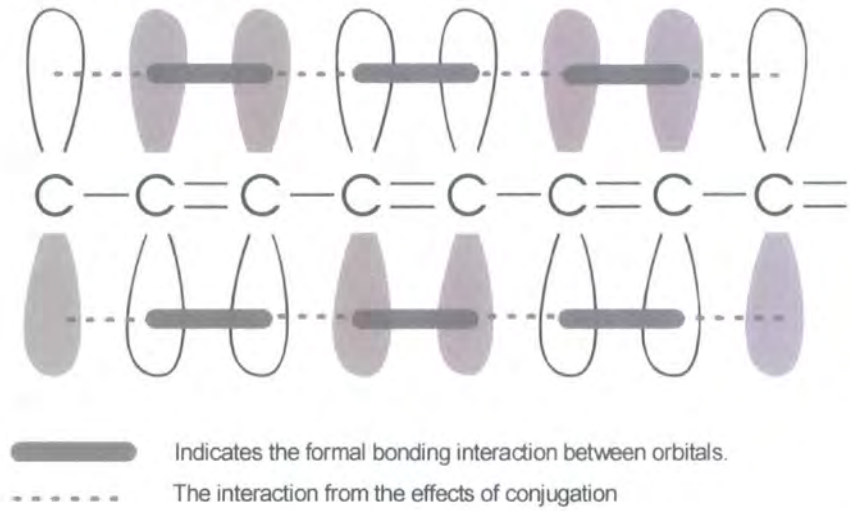

Figure 1.3 The effects of conjugation on the HOMO in the carbon backbone of the polymer polyacetylene.

Excitation types in conjugated polymers

Since detailed investigations into conjugated polymers began there have been many discussions about the nature of the excitations in the polymer. It was first proposed by Su, Schreiffer and Heeger et al that the excitation may be similar to that in inorganic semiconductors[11, 12], with the properties determined by electron-phonon interactions in the ground and excited states with little attention paid to electron-electron interactions. This led to charge carriers known as solitons, polarons and bipolarons travelling freely in valence and conduction bands in a similar way to inorganic semiconductors. However the more advanced thinking is that initially proposed by *Bassler et al* that the excitation is localised to a short length of the polymer chain, within this premise the excitation is considered to be a molecularly bound electron hole pair, an exciton[13]. The exciton can be formed either by absorption of a photon: photoexcitation, or by charge trapping; which occurs in electroluminescent devices. Once formed the excitons are able to move about the conjugated polymer until they decay with the release of a photon. Excitons can be characterised into three different types[14] depending on the size of their binding energy which is a result of the separation of the electron and hole often defined in terms of molecular crystals. The most bound excitons are known as Frenkel excitons, essentially the electron and hole are both localised on the same molecule or molecular unit. Charge transfer (CT) excitons have an electron and hole separated by similar distance to the separation of the molecules in the crystal, an electron has been effectively transferred from one molecule to a neighbouring one. The third type of

exciton, the Wannier exciton has the electron and hole separated by a large distance and correspondingly the electron and hole are less strongly correlated, this allows for the possibility that the electron and hole are not even present on the same polymer chain, this is known as an intrachain exciton.

Polarons

It is also possible to generate uncorrelated charges in a polymer chain, either through charge injection in a device[15], doping[16] or through the disassociation of weakly bound excitons (which naturally forms a pair in order to conserve the overall charge of the system). A charge on a polymer chain will induce a structural relaxation of the chain, effectively interacting with a phonon; this is known as a polaron[14], a single charge in an orbital such as this forms the SOMO defined earlier. The formation of a polaron and the structural change associated with it changes the level of the HOMO, SOMO and LUMO as a result polarons are characterised by two new allowed electronic transitions along with one spin forbidden one these are shown in figure 1.4. Two oppositely charged polarons in a material can meet and become bound by the coulomb interaction, known as charge capture, giving rise to a polaron pair. Polaron pairs can also be formed from a photocreated singlet exciton known as a geminate polaron pair[17]. After formation polaron pairs decay to excitons which then can undergo a radiative decay. This radiative decay is thought to be one source of the phenomenon of delayed fluorescence.

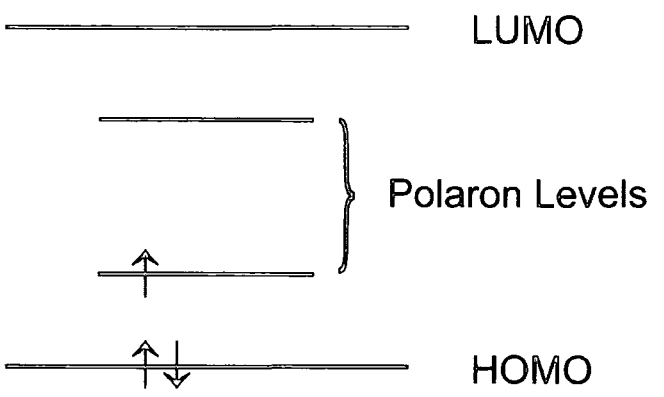

Figure 1.4 The extra states that polarons give rise to.

Singlet and Triplet Excitons

The nature of the electron and hole means that each have a spin and the conventional quantum mechanical model of bound fermions allows for the formation of excitons of two different spin states, singlet and triplet, the formation of the two states is shown in equation 1 below. As the ground state of conjugated polymers is known to be a singlet state, excitation by absorption of light can only produce singlets, the photon has no spin and spin must be conserved under excitation, therefore only a singlet excited state can be formed initially. Charge trapping in devices creates both singlets and triplets, statistically 75% triplets should be formed, as shown by equation 1, however there are still discussions as to the actual ratio of singlets to triplets formed after charge trapping[18, 19]. This is of particular importance because of the singlet ground state, triplets very weakly decay radiatively to the ground state due to spin conservation thus a 75% triplet generation rate represents a considerable loss of efficiency in devices. Although quantum mechanically forbidden triplet states can still be formed after photoexcitation of the sample through a process known as intersystem crossing; this is effectively a spin flip of the electron, a spin-orbit interaction with the

nucleus of an atom provides enough of a perturbation to allow it to take place for a small proportion of the excitons. Spin forbidden phosphorescence decay has been observed in many conjugated polymers[20, 21], both at low and room temperatures, this has a long lifetime of ~1s and a low quantum yield, compared with a high quantum yield and fast decay ~400ps for the singlet exciton. The emission is also considerably redshifted; typically about 1eV compared to the singlet emission; and as such is impractical for LED applications. This lowering of energy of the triplet state compared to the singlet is a result of the spin exchange integral. As the two electrons in a triplet state have the same spin, they have a greater repulsion between them due to the spin exchange integral, so are physically further apart than the in the singlet excited state where the opposite spins would allow occupation of the same space. The greater distance between the electrons reduces the electronic repulsion and hence the energy gap. As intersystem crossing is an isoenergetic process, once the triplet state is formed it undergoes a non radiative vibrational relaxation to the lowest lying triplet level.

$$Singlet = \frac{1}{\sqrt{2}}\left[(\uparrow\downarrow)-(\downarrow\uparrow)\right]$$

$$Triplet = \begin{cases} (\uparrow\uparrow) \\ \frac{1}{\sqrt{2}}\left[(\uparrow\downarrow)+(\downarrow\uparrow)\right] \\ (\downarrow\downarrow) \end{cases} \qquad \textbf{(Equation 1)}$$

Excitons in Conjugated Polymers: Energy Transfer, Quenching and Dynamics

The previous section has discussed the formation and radiative decay of excitons in conjugated polymers it is now time to look at the complex processes that

can take place within the envelope of the exciton's radiative lifetime. If we first consider the singlet, with its generally short ~1ns lifetime, has the simpler life of the two excitons, one of the most important process that the singlet undergoes is energy transfer.

Förster Energy Transfer (Resonance energy transfer)

The theory of Förster[22] energy transfer is based around the transfer of energy between two dipoles. The donor dipole, oscillating at its resonant frequency, energy from this oscillation is transfers its energy to another acceptor dipole of similar resonant frequency. The resonant frequencies of the donor and acceptor dipoles are quantified by their emission and absorption spectra. Thus, if the emission spectrum of the donor overlaps with the absorption spectrum of the acceptor energy transfer is possible. However this is not the only condition necessary for energy transfer, as we are dealing with oscillating dipoles which have an orientation therefore it is easily prooven that crossed dipoles cannot undergo energy transfer. The other fact affecting the rate of energy transfer is of course the distance between the two dipoles. We define this formally by the Förster radius, which is the distance at which Förster energy transfer competes equally with the radiative decay of the exciton. With these conditions in mind it is possible to from an expression for the rate of energy transfer, as follows.

$$k_T(r) = \frac{Q_D \kappa^2}{\tau_D r^6}\left(\frac{9000\ln(10)}{128\pi^4 N n^4}\right)J(\lambda) \qquad \textbf{(Equation 2)}$$

In this case k_T is the rate of energy transfer, r is the separation of the species, Q_D is the luminescence quantum yield of the donor molecule (in the absence of the acceptor), n is the refractive index of the medium, N Avogadro's number, κ^2 is a measure of how the dipoles are oriented with respect to one another (for randomly oriented dipoles κ^2 = 2/3) and τ_D the lifetime of the donor. The final part is $J(\lambda)$ which is known as the overlap integral and it expresses the degree of spectral overlap between the absorption and emission spectra of the acceptor and donor respectively. It is important to remember that even though the absorption and emission spectra overlap there is no photon involved in the energy transfer process; this is not just a case of emission and reabsorption. Typical values for R_0 the critical distance for energy transfer are generally a few nm, for example[23] for energy transfer from pyrene to coumarine the critical distance is 3.9nm and from the biomolecule tryptophan to pyrene the crytical distance is 2.8nm.

Forster transfer allows the singlet excitons to move relatively large distances between the polymer chains, there is one special case of this which results in a slightly unusual phenomenon; this is Singlet-Singlet annihilation, SSA.

Singlet-Singlet Annihilation

In SSA when two singlet excitons become close enough to interact the energy from one is transferred to the other, thus exciting the acceptor exciton to a higher state, and the donor returning to the ground state. The acceptor then thermalises emitting

phonons, leaving only a singlet excited state. Thus two singlets have annihilated with one another to form a single singlet, as follows.

$$S^1 + S^1 \rightarrow S^n + S^0 \rightarrow S^1(+S^0 + \Omega) \qquad \textbf{(Equation 3)}$$

As outlined previously one of the most significant processes that the singlet can undergo is intersystem crossing to the triplet state. This is effectively the flipping of the spin of an electron forming a triplet exciton rather than a singlet; it is caused by the spin orbit coupling of the nucleus allowing a relaxation of the spin conservation rule. Intersystem crossing is also enhanced in excitations which involve a change in the orbital angular momentum quantum number for example in an n-π* transition. Naturally the larger the nucleus of the atoms involved, the greater the spin orbit coupling and hence the greater number of triplets produced; this is the theory behind the phosphorescence emission of heavy metal dyes. The heavy metal effect is conventionally believed to only have an effect over short ranges. However, we have recently observed the interaction over a much larger distance.

Triplet Energy Transfer and Migration

Forster's theory of energy transfer must be extended to allow for dipole forbidden transfers such as those involving triplet states, this was done by Dexter[24] in his theory of electron exchange transfer, this is a relatively simple process whereby the electronic orbitals are close enough to physically overlap and thus an electron is exchanged from one to another effectively moving the exciton. In an energy transfer

reaction the Wigner spin selection rules mean that the spin and symmetry of the states must be conserved; in order that spin is conserved in triplet energy transfer it is necessary for 2 electrons to be exchanged between the orbitals.

As conjugated polymers are a disordered system they do not necessarily have a set of discrete energy levels, but a distribution of states[25, 26], this is conventionally modelled as a Gaussian distribution of states and the site energies are given by the following expression.

$$g(E) = \frac{N}{\sqrt{2\pi\sigma^2}} \exp\left(\frac{-E^2}{2\sigma^2}\right) \qquad \textbf{(Equation 4)}$$

E is the energy difference from the centre of the distribution; N is the total concentration of states, and σ the width of the distribution. The migration of triplets within the triplet DOS is strongly effected by the position of the DOS with respect to the thermal energy of the system, if the DOS lies below k_BT, then the triplets are free to move in all areas of the DOS, non dispersively, i.e. without the loss of thermal energy. Conversely if the DOS lies above the thermal energy of the system, for example at very low temperatures, the triplets migrate to the lowest states in the DOS loosing thermal energy until they can go no lower, at which point they move non dispersively amongst the lowest states[26, 27]. For most cases the thermal energy lies within the DOS and there is dispersive migration followed by non dispersive motion. As a result of this phenomenon the diffusion of triplets throughout the medium generally becomes time and temperature dependant, there is an initial period of

dispersive diffusion followed by a period of equilibrium diffusion, the turn over time for these two processes being temperature dependant.

Triplet –Triplet Annihilation

As with singlets, once migration is possible annihilation between two species becomes possible, effectively the triplets migrate until they collide and an electron is transferred from one to the other via the Dexter transfer process, forming an intermediate pair.

$$T^1 + T^1 \rightarrow (T^1 + T^1)^{1,3,5} \rightarrow (S_0 + T_n), (S_0 + S_n) \qquad \textbf{(Equation 5)}$$

As the intermediate pair involves two triplet states and consequentially 4 spins it can form in 3 ways, with singlet, triplet or quintuplet multiplicity, the end product is either an excited triplet or an excited singlet, depending on the multiplicity of the intermediate. The excited singlet then thermalises and forms the first excited singlet state which can radiativly decay, one source of the phenomenon of delayed fluorescence[27, 28] (DF). As TTA is governed by the migration of triplets, the effects of dispersive and non dispersive migration throughout the triplet DOS can often be seen in the rate of annihilation of the triplets and hence the decay of the DF.

Singlet Triplet Annihilation

In the same way that excitons of the same spin character can annihilate with on another, singlets and triplets can annihilate together. The mechanism for this is similar to singlet – singlet annihilation with a Förster like energy transfer from the excited singlet to the excited triplet. Thus the singlet emission and the triplet-triplet absorption (photoinduced absorption) must overlap, although it could be a higher energy excitation of the triplet than that commonly observed.

$$S^1 + T^1 \rightarrow T^n + S^0$$ **(Equation 6)**

Then follows the thermalisation of the triplet excited state.

$$T^n + S^0 \rightarrow T^1 + S^0 + \Omega$$ **(Equation 7)**

Exciton Quenching Mechanisms

Quenching describes any process which decreases the intensity of the emission of the sample, both the singlet emission and the triplet emission can become quenched. The mechanism of quenching is normally an unwanted energy transfer process, for example energy transfer to a non-radiatively decaying state. As this is an energy transfer between two species it naturally becomes a question of diffusion[29, 30], the quenchers can diffuse around the sample as the excitons migrate in the same area. As a result when mobility is reduced at low temperatures, the quenching becomes less of a problem.

Both singlet and triplet excitons can be quenched by on chain defects in conjugated polymers, one of the most common quenching processes of this type is the quenching of emission of polyfluorene derivatives by ketone[31, 32] groups on the polymer backbone which arise from photoxidation of defects created during the synthesis.

One of the most important quenchers for triplets is oxygen. Oxygen, being paramagnetic has a triplet ground state thus energy transfer to any triplet oxygen in the solution is a problem when measuring triplet lifetimes. For this reason measurements of triplet lifetimes are always made in solutions with the dissolved oxygen removed.

Calculation of Photoluminescence Quantum Yield

Quenching of excitons in conjugated polymers leads to a loss of luminescence efficiency. The photoluminescence quantum yield is an important measure of the emission efficiency of a polymer. It is essentially the ratio of the number of photons absorbed by the sample to the number emitted. As this is an experiment that relies heavily on the equipment used to collect the emitted light as well as to measure the amount of light absorbed; when calculated for solutions it is normally performed using a known standard as a reference to compare with the polymer under study. The following formula is then used to calculate the quantum yield of the polymer.

$$Q = Q_R \frac{I}{I_R} \frac{A_R}{A} \frac{n^2}{n_R^2}$$ **(Equation 8)**

Where Q is the quantum efficiency of the polymer Q_R is the quantum efficiency of the reference solution, I is the integrated fluorescence of the polymer, I_R is the integrated fluorescence of the reference, A and A_R are the optical densities of polymer solution and reference and n and n_R are the refractive indices of the polymer and reference solutions respectively.

As the only loss of efficiency is from non radiative decay channels quantum efficiency can be related to the rates of decay of the radiative and non radiative processes that are causing decay of the singlet.

$$Q = \frac{k_{rad}}{k_{rad} + \Sigma k_{nr}}$$ **(Equation 9)**

In this case k_{rad} and Σk_{nr} are the radiative decay rate and the sum of all the non radiative decay rates, which includes internal conversion, intersystem crossing and all the effect of all quenching mechanisms respectively.

Chapter 2 : Experimental Methods

The previous chapter has described how atoms bond into large conjugated molecules and how the resulting system has an energy level structure. In order to understand the photophysical properties of the polymers in devices it is necessary to understand fully the energy level structure and the relationships between processes that the excitons are involved in, this is done using a number of techniques, absorption, fluorescence, phosphorescence and photoinduced absorption.

Theory of Absorption, and Emission of Light

As the fundamentals of photophysics: absorption and emission spectroscopy are extremely well known and well used techniques. Absorption works on the principal that photons cause an electronic excitation of the molecule when light of the correct energy is incident on the sample. In an organic molecule this energy is required to promote an electron from the HOMO (highest occupied molecular orbital) to the LUMO (lowest unoccupied molecular orbital) or higher antibonding orbital. However, in many molecules this presents a problem, often the energy gap is too great for UV or visible light to cause the transition, this is because the electrons in the σ–backbone of the molecule are so tightly bound that the σ–σ^* transition is rarely possible with UV/Vis spectroscopy. The only transitions that are possible are π–π^* and n-π^* that is an excitation of either the π – electrons or the nonbonding (n-) electrons. This makes absorption spectroscopy particularly useful when studying molecules with double bonds, such as conjugated molecules. There is however, an additional consideration to

be taken into account with absorption spectra, this the effects of coupling of molecular vibrations on the electronic transition. At all temperatures molecular bonds are able to vibrate; these vibrations can couple with the electronic transition producing a series of additional energy levels above the ground state and excited states. Figure 2.1 shows how light can be absorbed by molecules in any of the vibration sub levels of the ground state and be excited to any of the vibrational levels of the excited state. If a simple diatomic model is considered, the vibrational levels are bounded by the potential energy characteristics of the ground and excited states of the molecules, as the diagram shows these do not necessarily occur with the same equilibrium bond length. The Franck-Condon principal[33] assumes that the electronic excitation occurs with no change in position of the nuclei, as the excitation occurs faster than the vibration ($<10^{-13}$s) of the bond, if the excited state does not have a suitable vibrational level with the nuclei in the same positions, bond disassociation occurs, the diatomic splits. However, in most cases the excitation occurs between two vibrational levels as shown in the diagram the excitation then usually relaxes to a lower vibrational state of the same electronic state, this is known as 'vibrational relaxation' after which the electronic state can drop back to the electronic ground state with the emission of a photon – fluorescence; hence the wavelength of the fluorescence is always longer than the wavelength of absorption. This energy loss through the relaxation of the molecule in the excited state is measured by the Stokes shift, which is the energy difference between the absorption edge and the fluorescence onset. The transitions between different vibrational levels give rise to the different peaks in the absorption and fluorescence spectra of each electronic transition known as 'vibronic fine structure'.

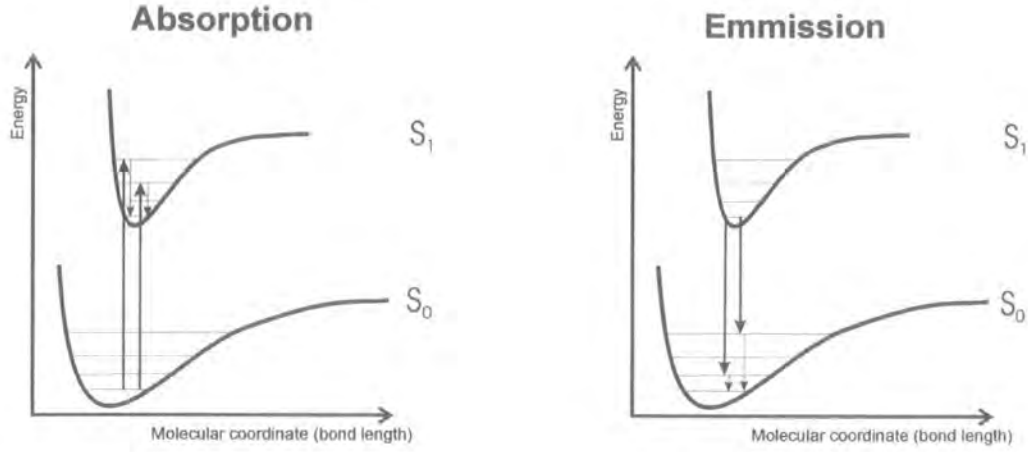

Figure 2.1 The Frank-Condon principal related to absorption and emission the thin lines represent vibrational relaxation of the state after absorption or emission of light.

The strength of the optical absorption can be described by a dimensionless property known as the oscillator strength[33] *f*, as defined in equation 10.

$$f = \left(\frac{4m_e c\varepsilon_0}{N_A e^2}\right) A = \frac{4.39\times10^{-9}}{n}\int\varepsilon(\bar{\upsilon})d\bar{\upsilon} \qquad \textbf{(Equation 10)}$$

Where m_e is the electron mass, c is the speed of light, ε_0 is the permittivity of free space, e the charge on an electron, A the integrated area of the absorption peak, n the refractive index a and $\varepsilon(\bar{\upsilon})$ the molar extinction coefficient of the sample in wavenumber units.

The oscillator strength is dependant on a number of selection rules which contribute to the overall probability of the transition. These rules govern the change in momentum, parity, symmetry and most importantly electron spin for allowed electronic transitions. The electron spin factor is of considerable importance as it prevents the direct photoexcitation and decay of triplet states. However, this rule can

be broken by the presence of a heavy atom in the system due to the influence of the large spin orbit coupling.

The proportion of incident light absorbed in a solution will depend on the amount of solution that the light passes through (the path length *l*) and the concentration of the absorbing species (*c*), this is known as the Beer – Lambert law[23]:

$$A(\lambda) = \log\left(\frac{I}{I_0}\right) = \varepsilon(\lambda)cl \qquad \textbf{(Equation 11)}$$

In this case $A(\lambda)$ is the absorbance or optical density of the sample, I is the intensity of the light after the sample I_0 is the incident intensity on the sample and $\varepsilon(\lambda)$ is the molar extinction coefficient of the solution expressed as a function of wavelength.

Absorption and fluorescence spectroscopy

Absorption spectra were recorded on a Perkin Elmer Lambda -19 spectrophotometer and fluorescence spectra on a Jobin Yvon Fluoromax – 3 spectrofluorimeter, which allows excitation of the sample at any point in the visible / near UV range.

Principals of Photoinduced Absorption

Photoinduced absorption spectroscopy is a technique used to investigate the higher electronic states of the molecule. It is particularly useful for the study of metastable states, in particular the triplet states of molecules. It is a pump probe spectroscopic technique, excited states are created by a pump beam; then the probe beam is used to measure the population of the states created. In the case of measuring the triplet population, singlets are created by direct absorption from the ground state of the molecule and then a small proportion of them are converted to triplets by intersystem crossing. The probe beam is then used to probe the absorption of the first triplet state; light is absorbed as the triplets are excited to a higher energy level, thus giving the photoinduced absorption spectrum. The transitions involved in photoinduced absorption spectroscopy are shown in figure 2.2. The small proportion (1-2%) of the number of excitations that form triplets can cause experimental difficulties due to the low triplet population and resulting small signal. Also if the triplets do not have a long lifetime there is very little triplet population to absorb the probe beam so the signals can once again be very weak. However, the lifetime can be increased by reducing quenching effects, particularly relevant to solutions, or by cooling the sample.

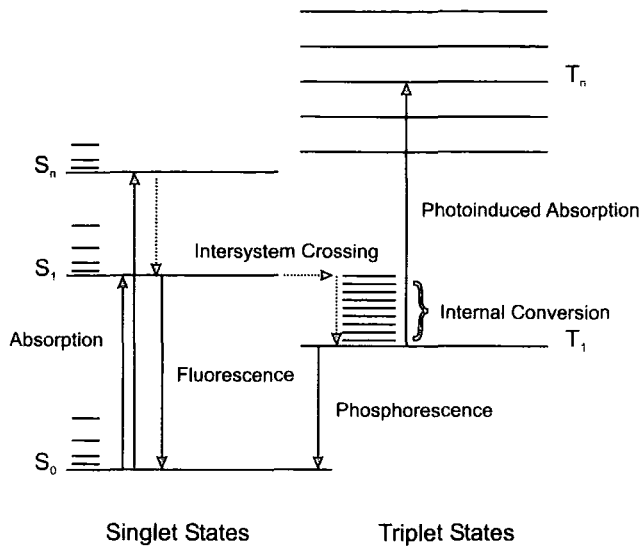

Figure 2.2 Jablonskii diagram showing the transitions involved in absorption, fluorescence, phosphorescence and photoinduced absorption.

One effect that can often be observed in photoinduced absorption spectroscopy that is not absorption itself is photobleaching. Photobleaching or ground state bleaching is a simple consequence of the long lifetime of the triplet state, this meta-stability allows the triplet population to accumulate; as the triplets do not decay immediately back to the ground state there becomes a point where there is reduced ground state absorption as there are considerably fewer molecules in the ground state available to absorb the incident light. This effect is seen on the PA spectrum as a negative signal (assuming the spectrum is displayed as an absorption spectrum rather than transmittance). It is generally only possible to see the photobleaching when the sample is pumped hard and the lifetime of the triplet is long, otherwise the ground state is replenished fast enough so that absorption is always possible.

Photoinduced Absorption Spectra Experimental Technique

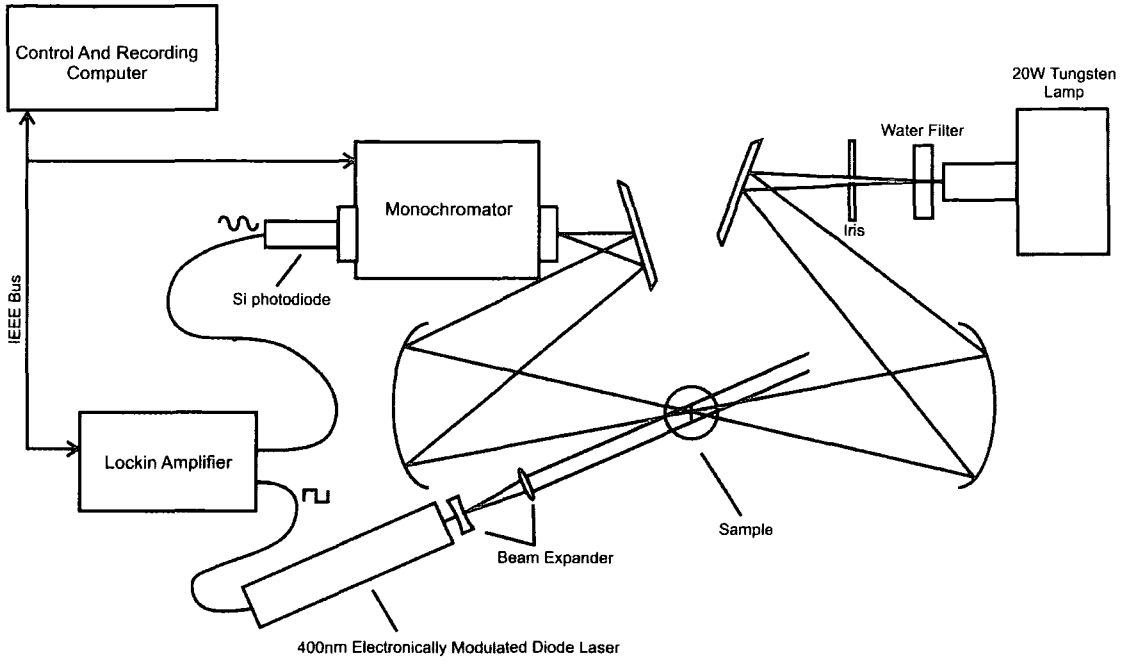

Figure 2.3 Experimental setup for quasi cw photoinduced absorption spectroscopy.

The method for investigating excited states using photoinduced absorption is now well established particularly the acquisition of spectra. The principal of the experiment is very simple[34], an intense laser beam is used to generate the excited state and then its absorption is measured using a white light, a monochromator and a photodetector just like in a spectrophotometer; figure 2.3 shows a diagram of the experimental setup. However, there are a few considerations that must be taken into account which make the experimental method more complex; the first of these is the ground state absorption spectrum, it is perfectly feasible that the white light probe beam is absorbed by the ground state as well as the excited state, this would result in a spectrum that is a combination of both the absorption and photoinduced absorption

spectrum, in fact, for the triplet states studied the ground state absorption will be far higher then the triplet absorption, due to the low number of triplets generated through intersystem crossing. The solution to this problem arrives through the use of a lock-in technique. The excitation beam is modulated (typically modulation frequencies are 10s of Hz), and the signal is detected using a dual channel lock-in amplifier. When the pump beam is off then the absorption is given by A(λ), when it is on the absorption is given by A(λ) + dA(λ) thus there are two components, a dc signal A(λ) and an ac one dA(λ). The lock-in amplifier picks out the ac component of the signal with the same frequency as the modulation frequency: the ac component dA(λ). This ac signal is the photoinduced absorption spectrum only. The nature of absorption by a species means that a proportion of the incident light is absorbed. However, as the lamp profile and response of the photodetector are not constant across the entire wavelength range it is necessary to scale the photoinduced absorption ac component by the dc component to yield the true photoinduced absorption. This is normally written in terms of transmission; *dT/T*. It follows that this is directly proportional to the number of excited states present, with the following relationship.

$$-\frac{dT}{T} = \sigma \frac{N}{A} \qquad \textbf{(Equation 12)}$$

Where, dT/T is the steady state photoinduced absorption signal, σ is the absorption cross section of photoexcitation (energy dependant), N is the total number of photoexcitations and A is the area of the excited sample exposed to the probe beam.

There is another advantage gained from using a lock-in amplifier; when the sample is excited, a broad fluorescence spectrum can often overlap the photoinduced absorption spectrum, thus obscuring the photoinduced absorption. This problem is not overcome by the modulation of the light as the fluorescence will occur at the same frequency as the excitation. However a feature of the dual channel lock-in amplifier is to give not only the magnitude of the signal at the same frequency as the reference (in this case the modulation of the excitation beam), it also give the phase difference between the reference and the signal channels. This phase angle (θ) allows us to split the spectrum into two components, one in phase with the reference, and one out of phase, these are given by the formulae below.

$$\left(\frac{dT}{T}\right)_{inphase} = \frac{dT}{T}\sin(\theta)$$
$$\left(\frac{dT}{T}\right)_{outphase} = \frac{dT}{T}\cos(\theta)$$

(Equation 13)

From these two components it is possible to separate the photoinduced absorption from the fluorescence. This is possible because the fluorescence lifetime of the polymer is negligible compared to the time period of modulation, so the fluorescence appears in only the in-phase component of the spectrum. The triplets studied have a much longer lifetime, which although is still not comparable to the time period of modulation is sufficient for their absorption to appear in both the in phase and out of phase components, thus it is possible to retrieve 'hidden' photoinduced absorption features from within the fluorescence spectrum of the sample.

Photoinduced Absorption Apparatus

The photoinduced absorption apparatus uses either the 457nm line of a Spectra Physics 2025 Ar+ ion laser and mechanical chopper or a 400nm electronically modulated GaN diode laser module for the pump beam (Laser 2000); the probe beam is provided by either a tungsten filament lamp or a xenon arc lamp. The tungsten lamp allows spectra to be recorded in the visible and near Ir region, whereas the Xenon arc lamp has emission further into the UV allowing absorption to be measured up to about 3.5eV. After passing through the sample the probe beam is monochromated by a Bentham monochromator before being detected by either a Si – photodiode for visible light or an InSb cooled detector for the Infra red. Both solution state and thin films spin cast onto sapphire or quartz substrates were used, temperature dependant measurements could be made on the films by cooling in an Oxford Instruments liquid nitrogen cryostat, allowing measurements to be taken at temperatures down to 77K. The apparatus also incorporates a water filter, which is used when spectra are being recorded in the visible and UV range in order to filter out the IR light to reduce the heating on the sample. Solution state experiments were made on solutions degassed using at least three freeze – evacuate – thaw cycles in a quartz degassing cell. The use of a TTL modulated diode laser as pump beam is slightly unconventional; however it holds many advantages over the mechanical chopper. Firstly it can be triggered directly by the lock-in amplifiers internal oscillator, which results in greatly reduced jitter and very stable chopping allowing the lock-in to 'lock' more easily, giving a more favourable signal to noise ratio. It also allows the use of considerably higher rates of modulation which can be useful when trying to resolve a noisy signal, this is particularly important when using the xenon arc lamp as probe source as the instability of the arc has a range of frequencies (1-100Hz) similar

to the mechanical chopper, thus preventing the lock-in amplifier from resolving the photoinduced spectrum properly. However, modulating the pump considerably faster (approximately 1kHz) than the instability of the arc prevents the noise from the lamp from obscuring the photoinduced absorption signal.

Time resolved PA

It is possible to calculate the decay lifetimes for the species identified in the photoinduced absorption spectrum by investigating the variation in signal intensity with chop rate. However, this requires some knowledge of the mechanism of the decay as a model must be first formulated and then mathematically manipulated into the same form as the chop rate dependence before the data can be fitted. Although this is easy enough for species which follow a simple first order kinetic scheme it is unreliable and unsatisfactory when more complex decays are being investigated, especially when there are multiple processes in competition. It is therefore necessary to use a more complex technique. In this investigation an electronically detected sub-nanosecond resolution pump-probe experiment[35] was used.

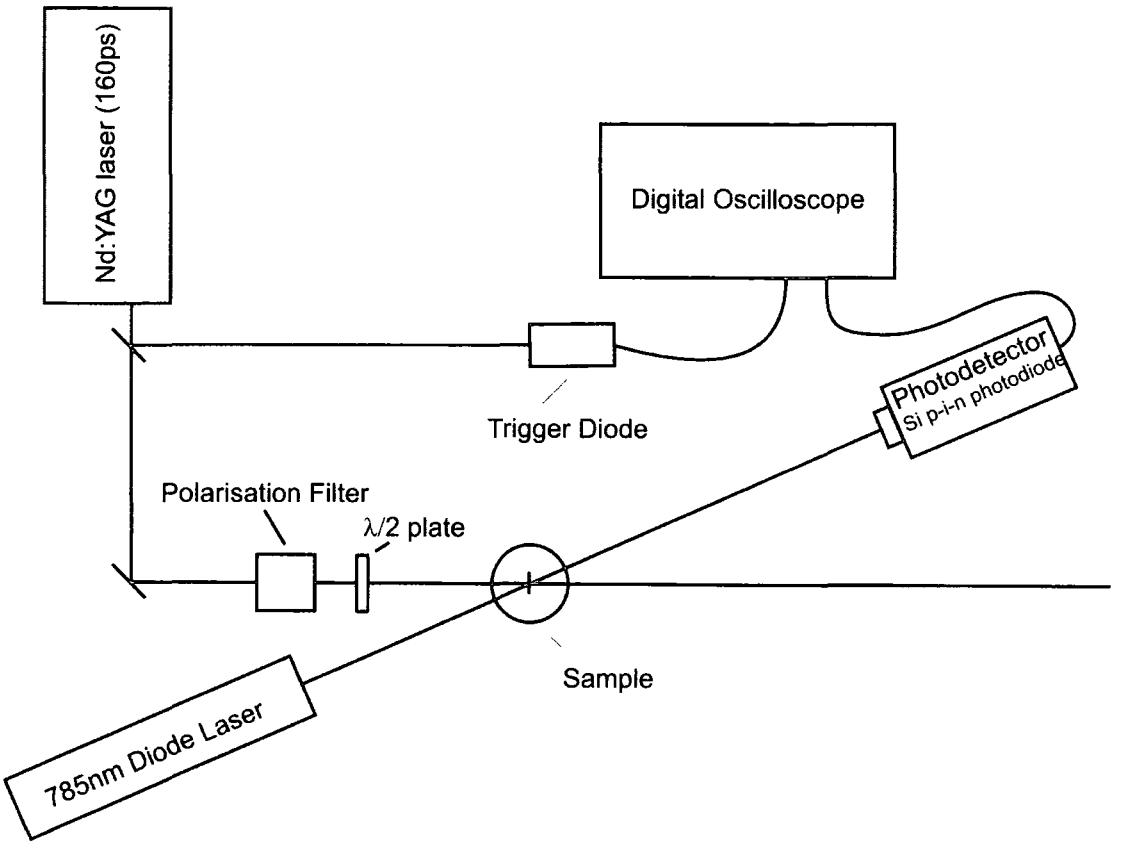

Figure 2.4 Schematic diagram of apparatus for time resolved photoinduced absorption measurements.

Fundamentally this experiment uses the same principals as the steady state photoinduced absorption spectroscopy experiments only in this case, a monochromatic light source is used as the probe beam and the temporal change of the signal strength at one wavelength is recorded. Apparatus for the experiment is shown schematically in figure 2.4. The pump beam provides an intense pulse of laser light to excite the sample after which the population of the excited species is monitored by a single wavelength probe beam. In order to preserve the true kinetics of the species this experiment requires the use of short laser pulses and detection electronics with a response comparable to the laser pulse length. The lower limit of the detection electronics limits the time resolution to approximately 500ps which allows the

investigation of most types of triplet behaviour in conjugated polymers, both fast and slow decays as well as the build in of triplets on some polymers.

The 3rd harmonic (355nm) generated line of a 160ps pulsed Nd:YAG laser (EKSPLA SL-312) was used as the pump beam and the probe beam was provided by a thermally stabilised and electromagnetically shielded diode laser which was chosen to be at the peak of the photoinduced absorption spectrum for the triplet state of the polymer under study. The use of a diode laser for the probe beam rather than the more traditional monochromated light source is very advantageous as it is no longer necessary to focus light after the onto the detector, in fact the detector was placed a considerably larger distance away than the small lens used to focus the beam onto the photodetector. This method minimises the collection of the fluorescence of the polymer by the detector, allowing us to improve temporal resolution to within the tail of the fluorescence, which can be problematic in the conventional experiments even when carefully selected cut off filters are used. Crucially this makes it possible to measure the build in of triplet states during the decay of the singlet. The experiment was set up in a collinear geometry, in solutions this makes the volume of interaction of the probe beam and the excited solution as large as possible thus maximising the photoinduced absorption signal strength and allowing signals at lower pump doses to be measured. The same arrangement proves perfectly satisfactory for thin film samples as well. Having passed through the excited solution or film the probe beam was detected using a $0.8mm^2$ silicon pin-diode built onto a 2GHz transimpedance amplifier (Femto Gmbh), the signal was then recorded using a 1GHz digital oscilloscope (HP Infiniuum), which was triggered directly by the pump laser via another pin diode. The entire detector setup allowed sub nanosecond time resolution

of the triplet kinetics, with a rise time for the system of under 500ps, having been measured as the response to the excitation laser itself.

Pump dose dependant studies can be undertaken by attenuating the excitation laser beam with a calcite polarisation filter and λ\2 wave plate and measuring the energy per pulse with a pulse power meter from which the pump power density was then calculated. It is also possible to change the excitation wavelength using a dye laser pumped by the Nd:YAG for excitation in different parts of the absorption spectrum. The experiment can be performed on samples in degassed solution or on thin films held in a closed cycle liquid helium cryostat, to allow temperature dependent studies down to 12K to be carried out. Films were held in the cryostat under vacuum even when room temperature experiments were carried out to ensure that the film was not degraded by the intense laser light in an oxygen containing atmosphere.

Time Resolved Fluorescence Measurements Using a CCD Camera

To complement the photoinduced absorption techniques, time resolved emission studies have been carried out using a gated intensified CCD detection system[27]. This allows the measurement of kinetics and spectra of fluorescence, delayed fluorescence and phosphorescence. A sample is excited using the frequency tripled 355nm line of the Nd:YAG laser, the emission is then dispersed through a monochromator onto a gated intensified CCD camera. The camera is triggered by the laser through a fast silicon pin diode and the delay time between the camera being

triggered by the laser and the recording of the spectrum can be varied. Combining this variation in delay time with a variation in the integration time for the spectrum acquisition allows the collection of the temporal change in spectra over signal intensities of up to 13 orders of magnitude; considerably larger than the actual dynamic range of the camera. The ability to resolve such small signals is in fact a very simple procedure, the gate time is merely increased along with the delay, so for long delays a longer integration time is used, and the data is then scaled appropriately to yield the kinetics. It is important to note that the gate time must be kept small compared to the delay time in order to yield the true kinetics, rather than the integrated kinetics, something that is not always possible when measuring very weak emissions particularly phosphorescence. The minimum time resolution of this system is 300ps, as this is the narrowest gate that the camera can accept. The spectral range is determined by the CCD which is sensitive between 300 and 900nm, and the monochromator allows us to disperse 300nm of the spectrum onto the CCD at a time. The grating can be moved to place different portions of the spectrum at the centre of the CCD.

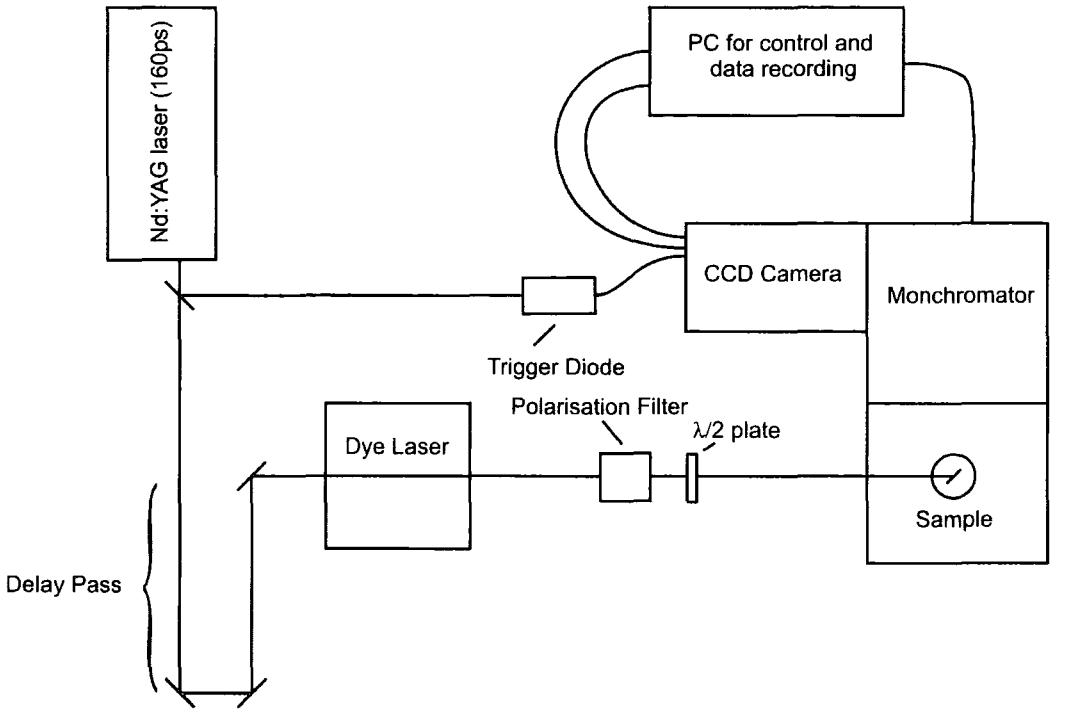

Figure 2.5 CCD camera for use in measuring delayed fluorescence and phosphorescence

The diagram in figure 2.5 shows the apparatus used, marked on the diagram is the optical delay pass, this is necessary because it takes approximately 30ns for the CCD camera to initialise after the trigger pulse, so in order that the initial part of the delayed fluorescence can be recorded it is necessary to build in a delay excitation of the sample. The diagram also shows a dye laser in the path of the excitation laser beam; which allows us to change the wavelength of the excitation which is particularly useful when dealing with blends of polymers and dyes. The calcite polariser and λ\2 plate is also present which as in the time resolved photoinduced absorption experiment allows us to change the intensity of the excitation for dose dependant studies. Experiments can be made using the same samples as the time resolved photoinduced absorption, degassed solution or thin films which can be held in the helium cryostat.

Chapter 3

Triplet Excitons in Polyspirobifluorene

Polyfluorene derivatives are one of the most promising classes of materials for PLED applications. Solution processable and highly efficient they can offer good blue emission and when copolymerised with other units can be adapted to emit throughout the visible range. The monomer structure is of two benzene rings coupled with an additional carbon which can be substituted to manipulate the solubility and photophysical properties, two of the most common polyfluorenes poly-9,9-dioctylfluorene (PFO) and poly(2,7-(9,9-bis(2-ethyl-hexyl)fluorene)) (PF2/6) are shown in figure 3.1 Their synthesis has been described in detail in the literature[36, 37]. One significant disadvantage is their lack of colour stability; when left exposed to oxygen the normally blue emission is significantly reduced with a yellowish green band appearing in the fluorescence spectrum. The source of this emission has been extensively investigated and it is believed to originate from a photooxidation reaction causing the formation of a ketone defect at the 9 position of the fluorene which quenches the emission. Recent developments in the understanding of the photooxidation process have resulted in the development of polyfluorene derivatives that are resistant to the formation of ketone group. One such derivative is polyspirobifluorene (PSBF), which has an additional fluorene unit substituted at the 9 position and is resistant to photoxidation. The structure of PSBF is shown in figure 3.2..

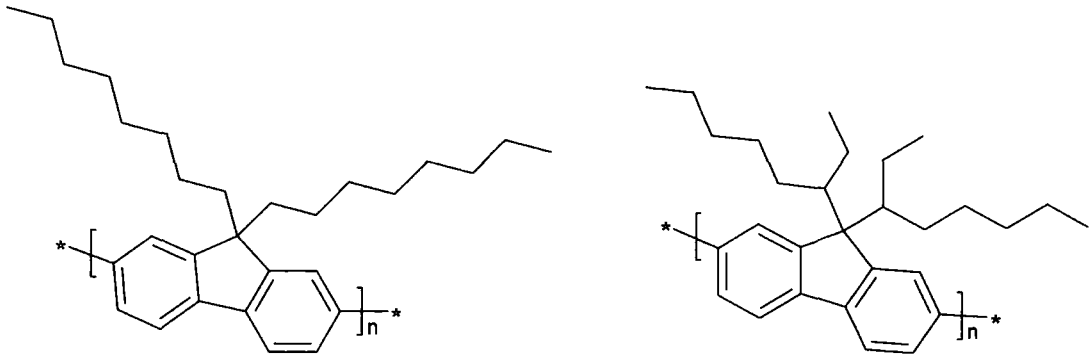

PFO PF2/6

Figure 3.1 The structures of some common polyfluorenes

The PSBF used in the investigation was synthesized by Covion Organic Semiconductor Gmbh; and is an unusually high molecular weight polymer, with a mean molecular weight of 770,000g/mol it is particularly good for photophysical characterisation as any quenching or other effects caused by the influence of groups at the ends of the chains are reduced. Another advantage of the increased length is that it is particularly suitable for studying intra chain processes, as it becomes more probable that there will be multiple excitons on each chain with increasing length.

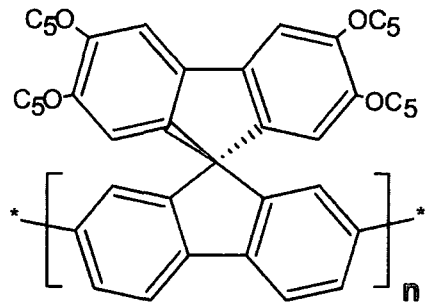

Figure 3.2 The structure of polyspirobifluorene (PSBF)

Isolated Chains In Solution

The room temperature solution absorption and fluorescence spectrum of PSBF are shown in figure 3.3, the fluorescence spectrum is very similar to that observed for other polyfluorene derivatives[28] although slightly red shifted by 0.06eV compared to PF2/6. The absorption spectrum however, does show a broader spectrum with an

additional peak at 3.6eV, which is attributed to the absorption of the unconjugated fluorene substitution; indicating that this Spiro derivative of polyfluorene has different photophysical characteristics to the more conventional aliphatically substituted polyfluorenes. The decay of the singlet state, measured by TCSPC (Time correlated single photon counting, a common technique for measuring fluorescence decays[38]) and shown in figure 3.4 gives an excellent fit to a monoexponential decay resulting in a fluorescence lifetime of 2.3±0.05ns, when measured at a concentration of 10^{-6} by weight in toluene. This is an unusually long lifetime when compared with other polyfluorenes, which is in fact very advantageous as the long lifetime makes it possible to measure the build in of triplet states through intersystem crossing as the singlet decays.

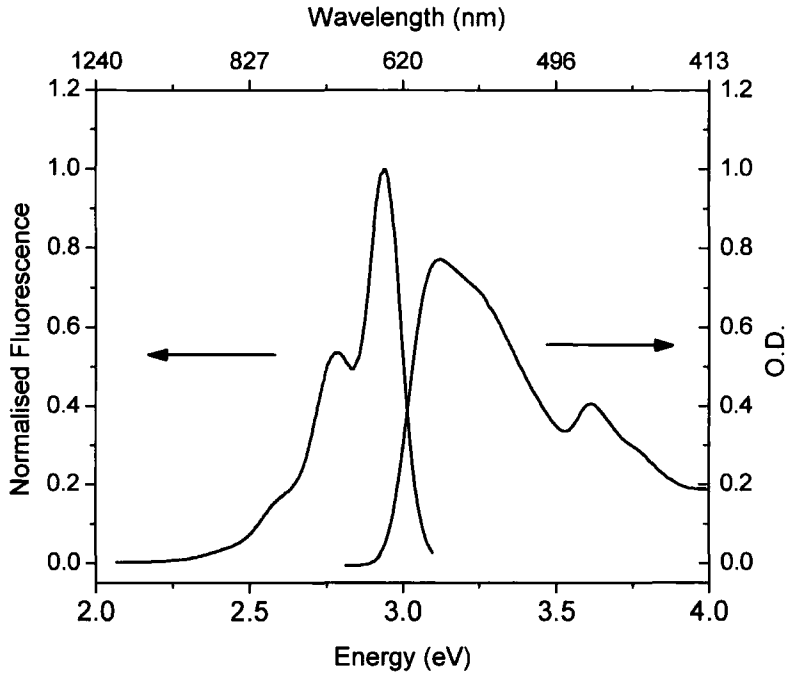

Figure 3.3 Absorption and fluorescence spectra of PSBF solution.

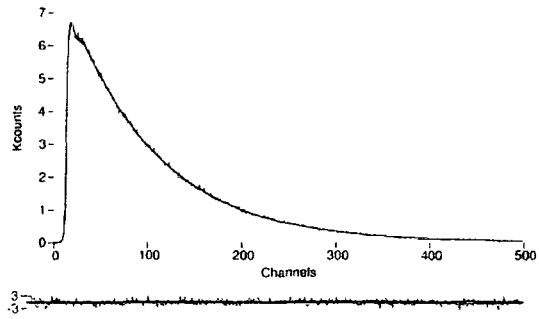

Figure 3.4 Singlet decay of PSBF solution as recorded by TCSPC the scale is 25ps per channel and the lower graph indicates the difference between the recorded data and the fit of 2.3ns decay time.

The photoluminescence quantum yield was calculated for polyspirobifluorene solution using the reference method outlined earlier with the reference solution as diphenylanthracene (DPA). In order to ensure that the measurement was as accurate as possible the solution of PSBF was made to have the same optical density as the DPA solution thus any errors due to nonlinearity of the instrumentation were reduced. Using this method gave a value of 0.93±0.05 for the photoluminescence quantum yield.

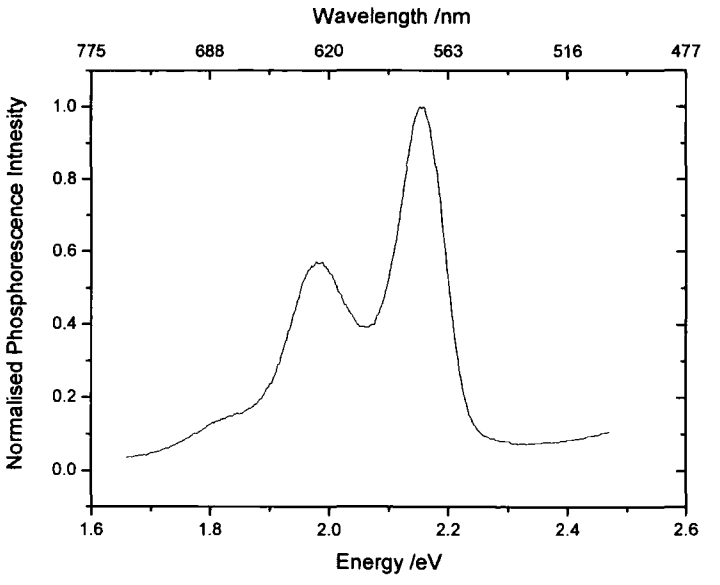

Figure 3.5 Phosphorescence spectrum of polyspirobifluorene film at 12K showing the triplet level at 2.16eV.

The energy level of the triplet state is characterised by measuring the phosphorescence spectrum which for thin films at 12K is shown in figure *3.5.* It is worth noting that it is not possible to measure the phosphorescence spectrum at room temperature. The data was taken with the time resolved emission experiment (CCD camera) using a delay time of 50ms after excitation and an integration time of 25ms. The peak at 2.16eV is the principal triplet level and it shows a second vibronic feature at 1.98eV; this corresponds to a redshift of approximately 0.71eV away from the singlet state. Figure *3.6* shows the room temperature solution steady state photoinduced absorption spectrum taken using the TTL modulated 400nm diode laser as pump source and the tungsten lamp as probe beam. The excitation power was 25mW over an area of approximately $0.75cm^{-2}$ which give an excitation power of $33mWcm^{-2}$. The data was taken with a chop rate of 23Hz and the polymer was at a

concentration of $1x10^{-5}$ by weight in toluene, placed in a 1cm path length quartz degassing cuvette degassed by 5 freeze-evacuate-thaw cycles.

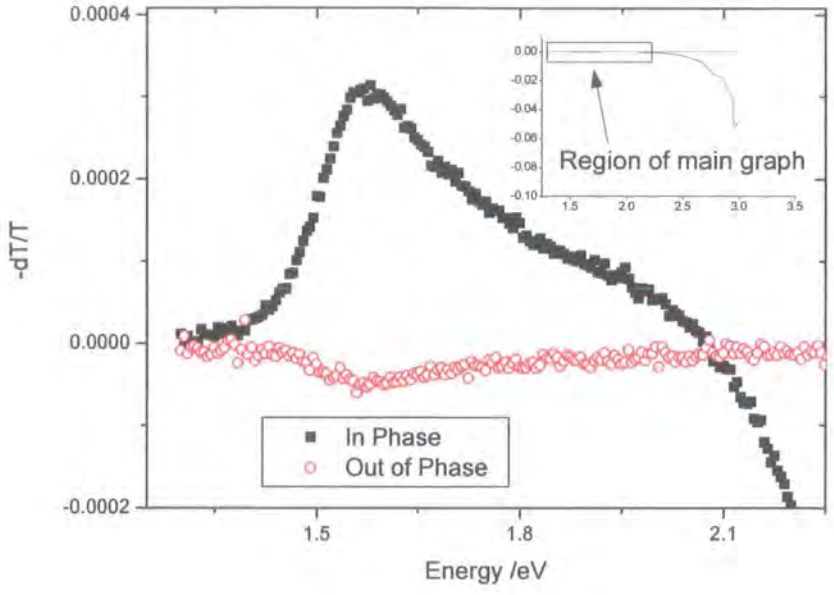

Figure 3.6 Photoinduced absorption spectrum of PSBF solution showing the triplet - triplet absorption at 1.57eV

The spectrum shows a peak at 1.57eV and a large trough shown on the inset at 3eV. The peak at 1.57eV is attributed to the photoinduced absorption of the triplet exciton and this is consistent with that observed for other polyfluorene derivatives, although a redshift of 0.04eV is observed when compared with PF2/6. The 3eV feature is attributed to the photoluminescence of the solution rather than the photobleaching of the ground state, this is due to the low energy tail, the ground state photobleaching spectrum should show the same shape as the ground state absorption, which has a steep edge on the low energy side and a tail on the high energy side

whereas the fluorescence spectrum has a steep high energy edge and a low energy tail, in the same way as the 3eV feature.

Triplet Build In

Figure 3.7 shows the change in time of the magnitude of the photoinduced absorption for the first 5ns after photoexcitation by the Nd:YAG laser at 355nm. The data was recorded with a toluene solution at a concentration of $1x10^{-5}$ by weight, it was not necessary to degas the solution for measuring such a rapid process because the diffusion time; that is the time it takes for a molecule of triplet oxygen to reach a triplet exciton; is longer than the time for the build in. The probe beam was a 785nm (1.56eV) diode laser which corresponds to the peak of the triplet exciton photoinduced absorption as measured previously in figure 3.6. This is verified by the fact that the number of triplets present is constant after the build in is finished.

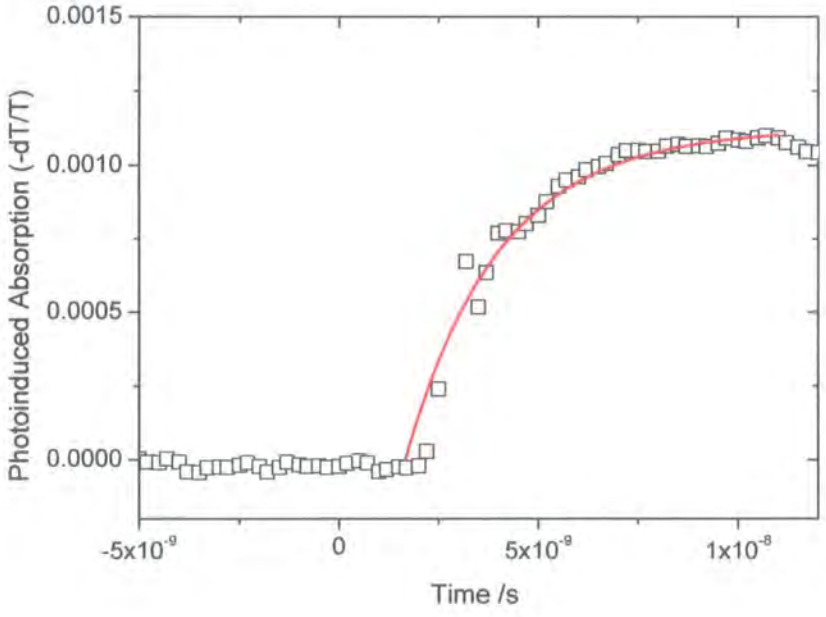

Figure 3.7 Build in of triplet states in a toluene solution of PSBF measured by time resolved photoinduced absorption

It is apparent that the rapid build of the signal and hence the number of triplet states does not occur solely within the 160ps laser pulse, thus the triplet build in is clearly a cold process, as expected a result of intersystem crossing from the first excited singlet state rather than direct photo-production of triplets. In fact the build in of triplets has almost exactly the same rate as the decay of the singlet. Using the intersystem crossing model for population of the triplet state it is expected that the triplet build in follows the decay of the singlet state, which is governed by the rate equation,

$$\frac{dN_s}{dt} = (-k_{nat} - k_{i.c.} - k_{isc})N_s \qquad \textbf{(Equation 14)}$$

this upon integration gives the number of singlets as.

$$N_s = Ge^{-(k_{nat}+k_{ic}+k_{isc})t} \qquad \textbf{(Equation 15)}$$

the rate constants k_{nat}, $k_{i.c.}$ and k_{isc} are the rates for radiative singlet decay, internal conversion and the intersystem crossing rate respectively; G is the singlet generation parameter, which is essentially the number of singlets generated by the laser pulse at time t = 0. This gives the rate equation and number of triplets for the process, assuming the slow decay of the triplets is insignificant in short time periods, as,

$$\frac{dN_T}{dt} = +k_{isc}N_S \qquad \textbf{(Equation 16)}$$

$$N_T = G\left(\frac{k_{isc}}{k_{nat} + k_{ic} + k_{isc}}\right)\left(1 - e^{-(k_{nat}+k_{ic}+k_{isc})t}\right) \qquad \textbf{(Equation 17)}$$

The photoinduced signal is proportional to the number of triplets; $dT/T = -\sigma n/A$, where n is the number of absorbing excited states, A is the sample area irradiated and σ is the absorption cross section. This can be combined with equation 17 and divided by A/σ and simplified as follows,

$$\frac{dT}{T} = C(1 - e^{-kt}) \qquad \textbf{(Equation 18)}$$

in this case C is the maximum of the photoinduced absorption signal and k is the sum of all the rate constants for all decay processes the singlet undergoes.

The data for the build in of the triplets after excitation with a dose of $300\mu Jcm^{-2}$, is fitted to the monomolecular build in formula (equation 5) yielding a value of $k = 4.2\pm0.2x10^{8}s^{-1}$, corresponding to a rise time of 2.4±0.2ns which is in excellent agreement with the 2.3ns decay of the singlet. The number of singlets only affects the total number of triplets produced after the build in has finished, as would be expected for consistency with the intersystem crossing model of triplet production. Other methods of population of the triplet state upon photoexcitation have been postulated, such as singlet fission[39] or geminate charge pair recombination[40, 41], we do not believe this to be the case for isolated polyspirobifluorene chains as this would require greater photon energy than our pump beam provides.

Decay of Triplet and Delayed Fluorescence

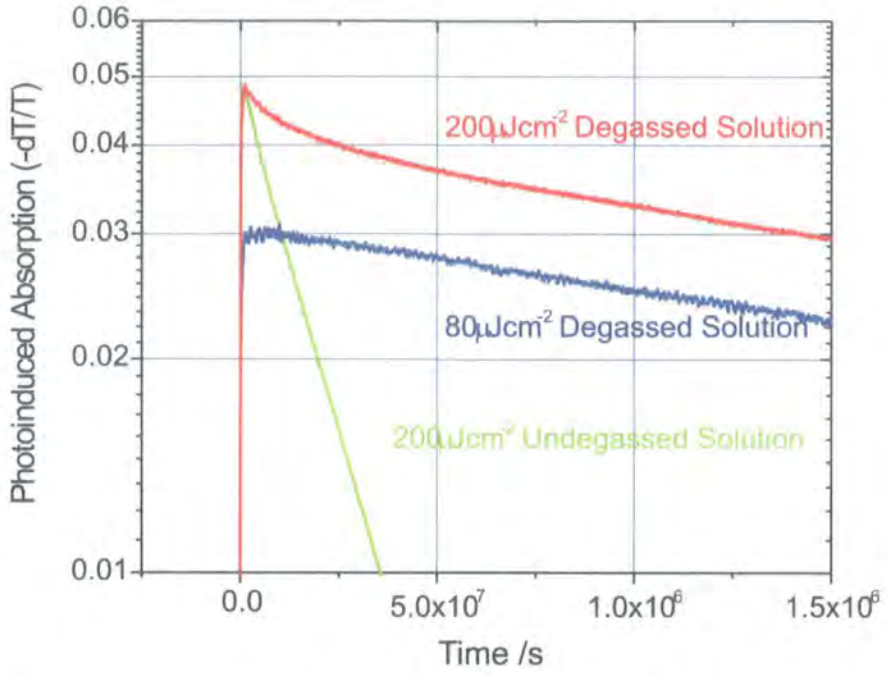

Figure 3.8 The decay of the triplet exciton for PSBF solution showing the presence of an additional fast decay mechanism for high excitation doses, as well as the effect of dissolved oxygen on the lifetime of the triplet.

The decay of the triplet in $1x10^{-5}$ by weight toluene solution as measured using time resolved photoinduced absorption is shown in figure 3.8. At low excitation laser doses (less than 100 μJcm^{-2}) in the degassed solution this exhibits slow monoexponential decay with a lifetime of 5.56 ms, this is as expected for a solution which is known to contain quenchers including water. When oxygen is present in the solution the lifetime is dramatically reduced to 254 ns, as has been mentioned previously this is due to energy transfer to the triplet oxygen ground state, a common quencher for the polymer triplets.

For higher excitation doses, greater than $100\mu Jcm^{-2}$, the triplet is observed to have an initial fast decay component, after which follows the same monomolecular decay as with the low dose case. This is visible in figure 3.8 and is found to be independent of concentration, with the fast decay process beginning at excitation doses between 50 and $100\mu Jcm^{-2}$. In order to quantify the laser dose dependence

better the laser dose dependence of the magnitude of the photoinduced signal after 100ns is plotted in figure 3.9 alongside the dose dependence of the maximum of the photoinduced signal after triplet build in. It is observed that for doses below 100μJcm^{-2} the number of triplets remaining after 100ns follows directly the number initially created and is directly proportional to the laser dose, as would be expected for a monomolecular decay route. At higher laser doses the number of triplets remaining diverges from the number initially created with a slope of 0.5 thus suggesting that the triplets are decaying with a rate that has a quadratic relationship to the number created. This is consistent with what would be observed for a bimolecular decay mechanism.

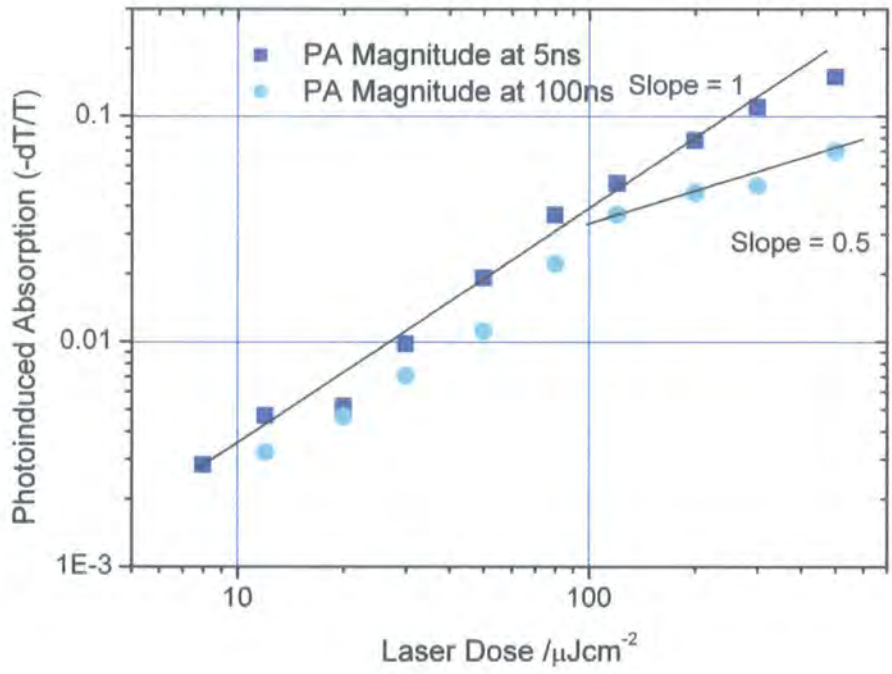

Figure 3.9 Dependence of the photoinduced absorption intensity after 100ns compared with the initial PA intensity for increasing laser dose. Slopes of 1 and 0.5 are shown for comparison the 'switch on' of a bimolecular decay process is clearly visible.

Having investigated the triplet kinetics through photoinduced absorption it became apparent that in solution state the triplets were undergoing more complex

processes than simply phosphorescence and quenching decays. One useful way of investigating these processes is to look at the delayed fluorescence of the polymer and to relate the delayed fluorescence to the triplet population. Figure 3.10 shows the spectrum of the delayed fluorescence alongside the prompt fluorescence.

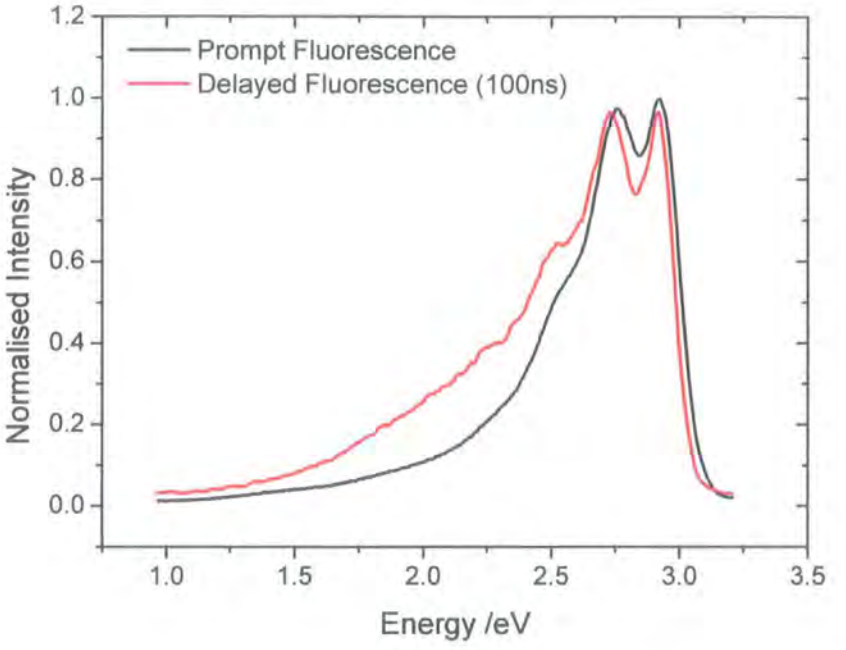

Figure 3.10 Fluorescence and Delayed Fluorescence of PSBF solution

The prompt fluorescence was measured from immediately after excitation with an integration time of 0.5ns and the delayed fluorescence was measured with a delay time of 100ns and an integration time of 10ns. In Figure 3.10 these data are normalised, which clearly shows that the delayed fluorescence arises from the decay of the same excited state as the prompt fluorescence; the first excited singlet state. There is a slightly different vibronic character in the delayed fluorescence compared to the prompt fluorescence. The decay of the delayed fluorescence are shown in figure 3.11, for excitation doses of $50\mu Jcm^{-2}$ and $200\mu Jcm^{-2}$. DF measurements also show the additional decay mechanism for excitation doses above $80\mu Jcm^{-2}$. This manifests

itself in the region of the higher excitation dose DF curve at times between 40 and 80ns delay, this is seen as an increase in the signal compared to the low dose DF measurement.

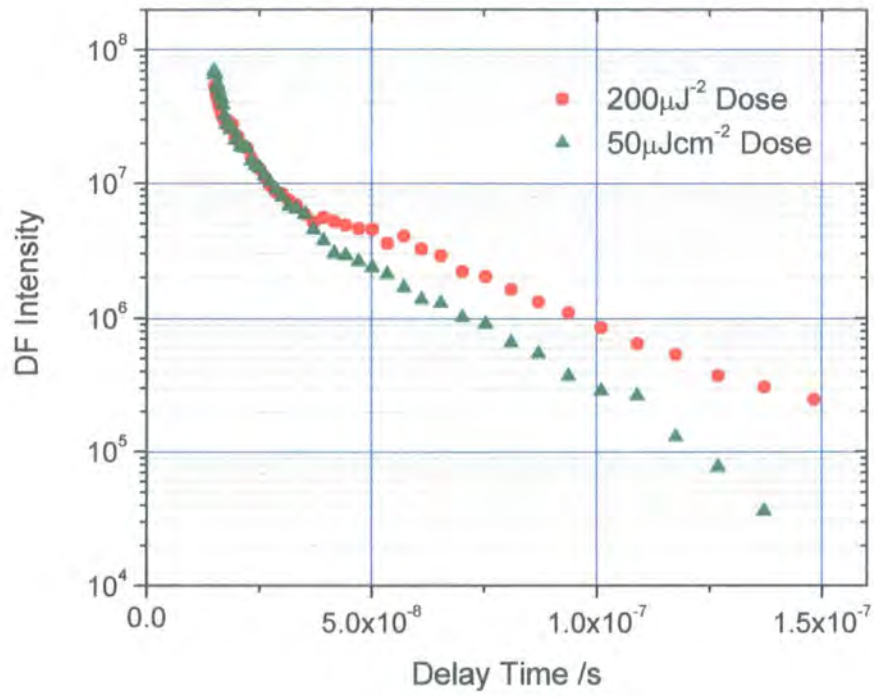

Figure 3.11 Decay of the DF at two different excitation doses showing a clear additional component to the DF for high laser doses.

Owing to the fact that the delayed fluorescence emission is proportional to the first derivative of the triplet population this indicates a more rapid decay such as a bimolecular process is taking place. The difference between the signals is small because there are other processes in addition to the rapid decay of the triplet contributing to the DF, such as diffusion controlled impurity quenching and geminate pair recombination. The same laser dose turning point in the decay mechanism is evident in the delayed fluorescence as shown in figure 3.12, recorded at a time delay of 100ns after excitation. The prompt fluorescence varies linearly with pump dose

throughout the experimental range. The delayed fluorescence however, varies quadratically for low doses but above about $100\mu Jcm^{-2}$ a linear dependence is observed. This is again consistent with a bimolecular decay mechanism at high powers, the bimolecular decay initially depletes the states rapidly so after a time interval the rate of decay and hence the magnitude of the delayed fluorescence is lower.

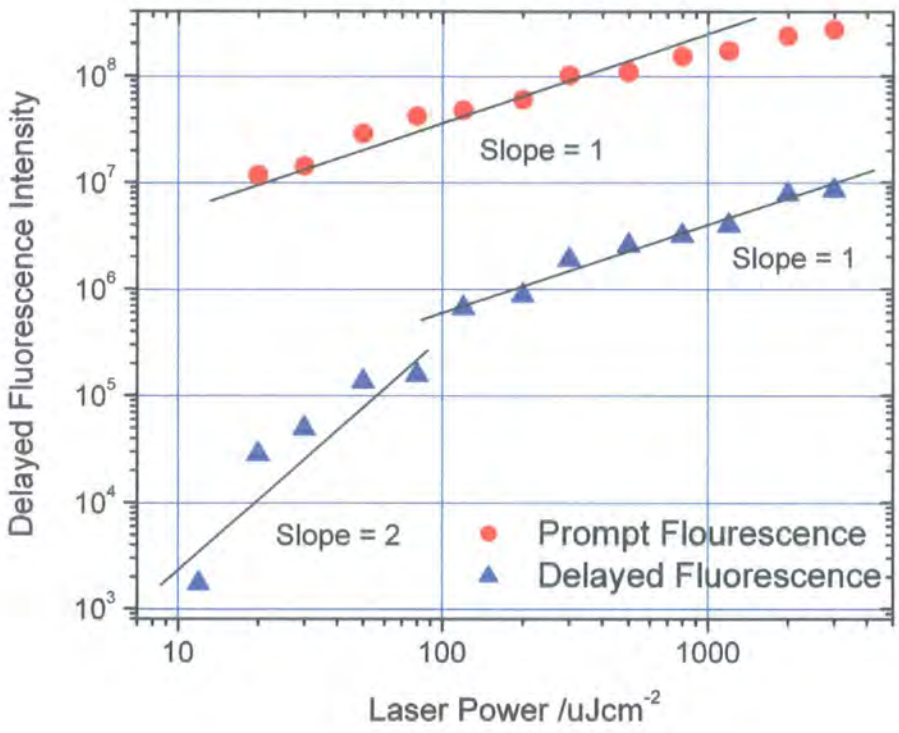

Figure 3.12 Comparison of the effect of increasing the laser dose on the prompt and delayed fluorescence. The turn over of the slope of the DF from 2 to 1 is a clear indication of the start of a TTA based contribution to the DF.

The presence of a bimolecular decay route suggests immediately an annihilation process; this remains a suitable conjecture for this case. Triplet – triplet annihilation (TTA) is most likely in this case as no bimolecular decay is seen in the prompt fluorescence which would be an indicator of singlet – singlet or singlet – triplet annihilation. Annihilation effects are often not present in dilute solutions such

as these, because this is considered to be the isolated chain regime, there is a low probability of interactions occurring between polymer chains. This leaves only the possibility of intrachain annihilation which is believed to be the case for this polymer. The lack of concentration dependence of the TTA decay acts to enforce this hypothesis, an inter chain process would undoubtedly be more prevalent at higher concentrations and hence show a faster rate, as the individual chains would come into contact more frequently allowing more annihilation reactions to take place. This cannot be present in an intrachain process as the rate of reaction will be dependant only on the density of excited states on each individual chain and the rate of migration of the states along the chains. Further confirmation of an intrachain process is given by the very presence of the change of decay mechanism; we postulate that the $80\mu Jcm^{-2}$ laser dose threshold is the point at which multiple triplet excitations appear on the individual chains. From this it is possible to calculate a lower bound on the intersystem crossing rate; if we take $80\mu Jcm^{-2}$ to be the turning point of the decay mechanism and assuming that at this point multiple triplets start to be generated on chains it is possible to calculate the ratio of triplets to singlets generated and assuming all triplet production is through intersystem crossing; calculate the intersystem crossing yield. The number of singlets on each chain is calculated by first calculating the amount of laser power absorbed and thus the amount of singlets generated in the solution dividing by the chain density then gives the singlet density per chain. The triplet density per chain is found by estimating the proportion of triplets that are quenched in annihilation reactions, although it is important to take into account the triplets produced as a result of the annihilations themselves. This gives a lower bound of 0.01 ± 1 which is realistic given the value of 0.03 calculated by photoaccoustic calorimetry for poly(9,9-dioctylfluorene)[42, 43]. The value remains an absolute lower

bound because there may be multiple excited chains where the triplets never meet to annihilate.

The general rate equation for decay of the triplets involving a bimolecular mechanism such as TTA in addition to a monomolecular quenching process is,

$$\frac{dN_T}{dt} = -k_T N_T - \gamma (N_T)^2 \qquad \textbf{(Equation 19)}$$

In this case N_T is the number of triplets; k_T is the monomolecular rate constant and γ is the annihilation constant. The photoinduced absorption data in figure 3.8 can be fitted to this using a competing monomolecular and bimolecular model, which for our data yields a value of $\gamma = 2.9 \pm 0.1 \times 10^8\ cm^3 s^{-1}$. Smoluchowski's theory of diffusion controlled reaction kinetics suggests that the annihilation constant would be dependant only on the diffusion coefficient, (D); the interaction radius (r) and the fraction of the triplets that annihilate on encountering each other (f), this gives[44],

$$\gamma = 8\pi fRD \qquad \textbf{(Equation 20)}$$

In the solid state this annihilation constant has been investigated thoroughly yielding more complicated results than this theory would suggest. The nature of the density of states in conjugated polymers leads to a theory that the interchain triplet hopping rate in three dimensions and consequentially D is time dependant, characterised by a rapid decay of D as the triplets dispersively relax towards the tail

states in the distribution of states, then follows a steady state constant value of D when the triplets have enough thermal energy from their surroundings to hop non-dispersively amongst the low energy states. The problem of relaxation to the low energy states has been solved analytically[45] and in the long time limit can be shown to approximate[46] to $\gamma(t) \sim t^{-1.04}$. The solution state time resolved photoinduced absorption data in this study shows no such dependence even though there is still a distrubution of states; in fact the time dependence which fits the data is $\gamma(t) \sim t^{-0.05}$. Although at first glance it seems that our data is inconsistent with this theory it remains perfectly valid. At room temperature, where our solution state experiments were performed, the number of states created above the thermal energy level is small, and thus the dispersive migration of triplets is very rapid. It follows that we only observe the non-dispersive migration of triplets within the density of states; essentially the steady state value of γ that at low temperature would be observed after the turning point in the decay mechanism. The turnover from dispersive to non-dispersive migration has been observed by *Rothe et al* in the solid state[27] and is investigated further in the second half of the chapter. It is important to note that the hopping in solid state is three dimensional, interchain in nature and there may be differences with the one dimensional intrachain migration observed in solution.

Finding a constant value for the annihilation rate allows the calculation of the hopping rate along the chains, to do this a number of assumptions must be made. Firstly, that there are only two triplets generated on each chain, as this is not necessarily true, making this assumption means that the hopping rate calculated is a maximum as with only two triplets generated per chain the distance between the triplets is maximised. The other assumption is that the triplets are unable to hop past

each other without annihilating, they simply move along the chain until they collide and annihilate; therefore using this simplified model the hopping rate is calculated using the equation

$$rate = \frac{1}{2} l \times \gamma \qquad \textbf{(Equation 21)}$$

l is the length of the chain and g the annihilation rate, the factor of ½ is included to allow for the fact that the two triplet excitons are not necessarily at the ends of the chains. Using this simple formula we can calculate the hopping rate to be approximately 10^9 nm s^{-1}

It is also important to note however the presence of triplet-triplet annihilation without singlet annihilation. This indicates that the intra chain singlet mobility is low in comparison to the triplet, especially when the number of singlets photo-created is almost two orders of magnitude greater than the number of triplets formed. Thus there would certainly be a high enough intrachain singlet density to cause annihilation even considering the much shorter lifetime of the singlet. This suggests that the singlets are considerably less mobile than the triplets along the chain, a result that has been suggested previously[47].

Triplet – Triplet Annihilation in Films of Polyspirpbifluorene

Investigating the processes in dilute solutions invariably leads to results for the simplest case, intra chain effects are only visible because of the separation of the chains. However, in PLED devices the polymers are no longer in solution, the chains are in contact with one another and as a result there are many interactions which can take place between the chains. These can be investigated with the polymer cast onto

sapphire substrates. As the films are solid it is also considerably easier to control the motion of the triplets; this is done by adjusting the temperature of the sample. When the polymer films are cold the triplets move so slowly that they do not find another triplet and annihilate before they decay through phosphorescence, with this in mind it is possible to control the rate of annihilation of the triplets.

Both time resolved transient absorption and delayed fluorescence measurements were carried out on thin films held on the cold finger of a closed cycle liquid helium cryostat. Along with these experiments it is possible to measure the phosphorescence of the polymer at low temperature, whose kinetics should follow exactly the time resolved transient absorption measurements. The absorption, fluorescence photoinduced absorption and phosphorescence of the films of polyspirobifluorene are shown in figure 3.13 and 3.14 when compared to the solution state measurements in figure 3.3 there is little difference. The absorption spectrum once again shows two features, one form the polymer chain and one from the fluorene unit substituted at the 9 position; the fluorescence spectrum is slightly red shifted compared to the solution state spectrum, giving an increase in Stokes shift on going from solution to the solid state. In the photoinduced absorption spectrum the triplet exciton is once again seen, this time at 1.53eV which represents a slight redshift in comparison to the solution.

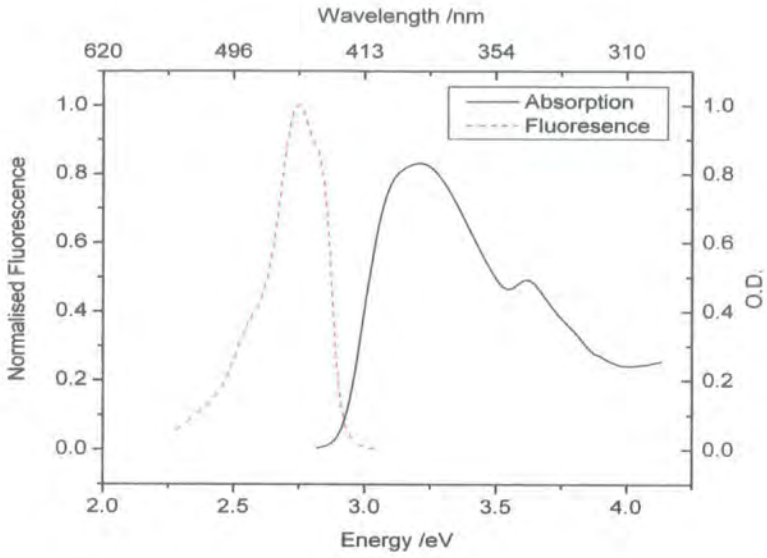

Figure 3.13 Absorption and fluorescence spectra of films of PSBF.

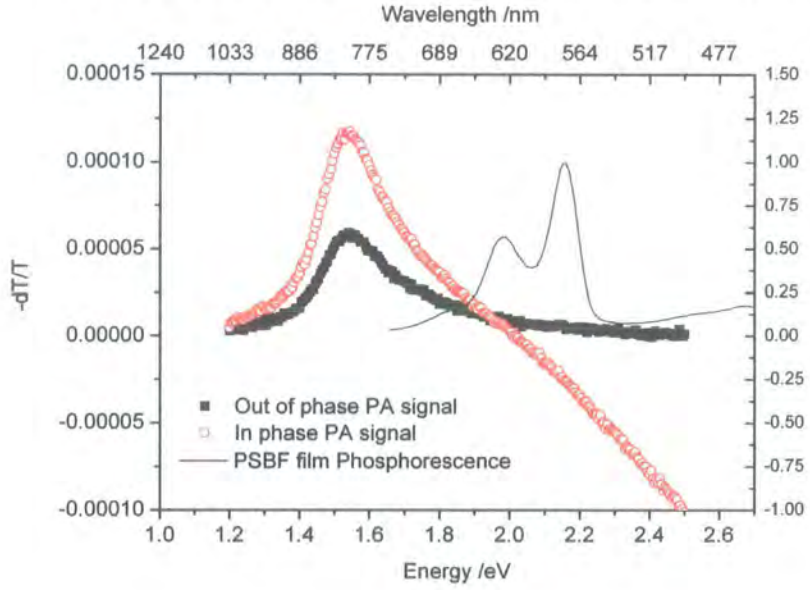

Figure 3.14 Photoinduced Absorption and phosphorescence spectra of PSBF films, the PA was measured at 80K and the phosphorescence at 12K.

The decay of the triplets as measured by time resolved photoinduced absorption is shown in figure 3.15 these data were taken at 160K and as with the solution data there is clearly two components to the decay, initially there is a non-exponential decay which is then followed by an exponential decay shown by the straight line on the semi-logarithmic plot. The exponential part of the decay fits well

to a lifetime of 2 ms, however this is merely a function of the temperature as the triplets are still able to move around and find quenching sites. As the other graph in figure 3.15 shows the lifetime is clearly increasing with decreasing temperature.

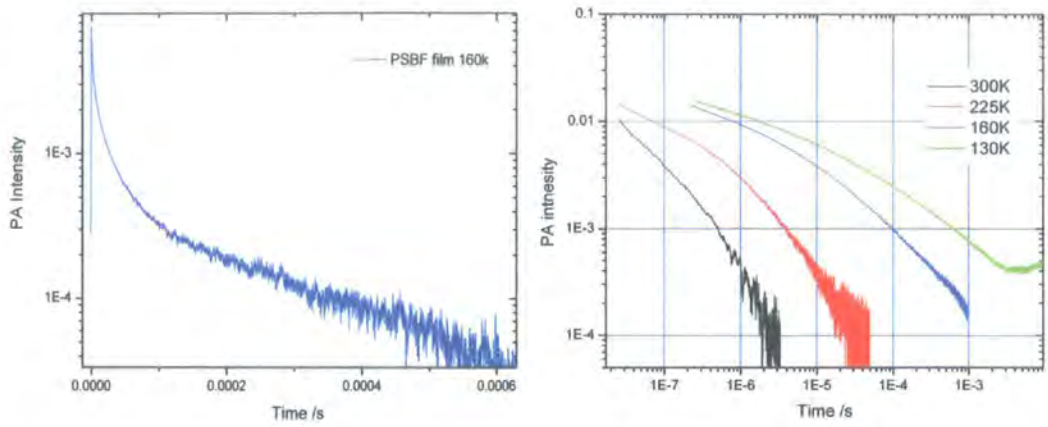

Figure 3.15 The left hand graph shows the decay of photoinduced peak of PSBF film at 160k. The other is the same decay at 4 different temperatures in a double logarithmic presentation, the data has been smoothed with a 25point adjacent averaging algorithm.

To try and understand the non exponential component it is once again necessary to look at the delayed fluorescence of the polymer, as figure 3.16 shows, this is a non exponential decay which shows an increasing lifetime as the film is cooled as would be expected from delayed fluorescence originating from triplets. In fact the straight line on a double logarithmic graph indicates that the decay is dominated by a power law before a change to a faster decay. The turnover to the faster decay is determined by the temperature, higher temperatures turn over faster.

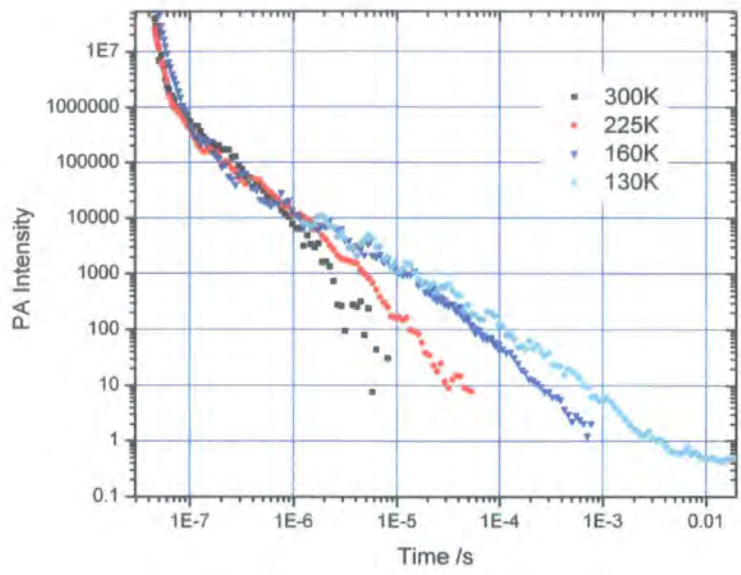

Figure 3.16 Delayed Fluorescence decay for PSBF films at various temperatures, the turning points between the two decays are clearly shown.

The source of the delayed fluorescence in conjugated polymers has always been a contentious issue. It is believed that in the methyl ladder type polymer, MeLPPP delayed fluorescence originates from delayed charge carrier recombination, on the other hand in PPV (poly(p-phenylene vinylene)) and PPE (poly(p-phenylene ethynylene)) it has been shown to originate from TTA. In polyfluorenes DF is attributed to TTA[27]; the investigation of the DF in polyspirofluorenes is clearly a natural progression from these studies.

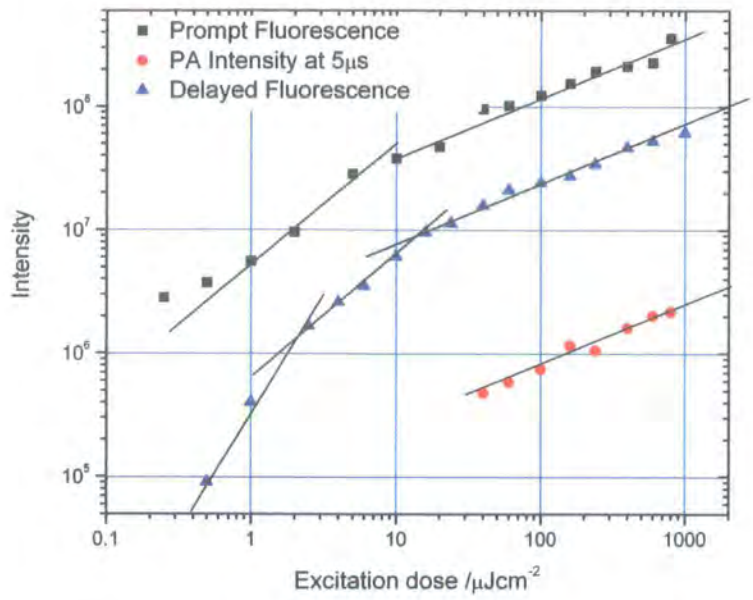

Figure 3.17 Excitation dose dependence of the photophysics of films of PSBF at 160K, the PA intensity has been scaled by 10^8 for clarity and the lines shown have gradients of 2, 1 and 0.5.

The two types of decay for the triplet once again point immediately to an annihilation process, in order to understand this better it is necessary to look at the dose dependence of the photo physics, this is shown in figure 3.17. The graph shows three important features, firstly in the photoinduced absorption data; there is no turn over at 100μJcm^{-2} like that found in the solution state experiments. In fact the gradient of the line is a constant gradient of 0.5, suggesting that the bimolecular decay has started for considerably lower pump dose. The second interesting feature is the presence of a change in gradient of the relationship between the prompt fluorescence and the excitation dose; this change form a gradient of 1 to 0.5 occurs at a pump dose of 10μJcm^{-2} . This change in gradient indicates that at high pump doses the singlets become involved in a bimolecular decay mechanism; the most likely conjecture for this has to be singlet-singlet annihilation suggesting that the singlets are able to move around in the solid state, which we must remember was not possible on isolated

chains in solution. The final interesting feature is the turn over in the gradient of the delayed fluorescence, this occurs at two separate points, firstly a turnover from a gradient of 2 to 1 at 2.5μJcm^{-2} and then a turn over from 1 to 0.5 at 10 μJcm^{-2}. These turn overs support the idea of singlet – singlet and triplet – triplet annihilation. TTA is responsible for the turn over at low pump doses and then at higher pump doses singlet-singlet annihilation begins, it is important to note that it is possible to see the effect of SSA in the delayed fluorescence, not because the singlets produced by the TTA are annihilating with one another, as in reality the spin statistics of recombination means that the number of singlets produced is too few, but because the number of triplets originally produced from intersystem crossing is affected by the SSA.

The fundamental differences between the annihilation process in solution and that happening in the solid state lies in the origin of the annihilating species. As described previously in dilute solutions the species lie on the same chain; however, in films it appears that both the singlets and triplets are able to travel around the film between the chains and annihilate. For singlet - singlet annihilation this must clearly be the case, as no SSA was seen in solutions, so the singlets are unable to move very far along the isolated chains, in the films they must be moving between the chains to annihilate. TTA in films begins at a much lower excitation dose than in isolated chains, at such a low dose, it is not likely that multiple triplet excitons are formed on each chain, therefore they must be travelling between the chains in order to annihilate.

In order to test the validity of the suggestion that at low dose the delayed fluorescence is due to TTA it is necessary to once again remind ourselves of the rate equation for decay of the triplets,

$$\frac{dN_T}{dt} = -k_T N_T - \gamma (N_T)^2 \qquad \textbf{(Equation 22)}$$

Where N_T is the triplet population, k_T is the rate of monomolecular decay and γ is the annihilation constant. In the regime of delayed fluorescence, (up to 1ms) we can neglect the monomolecular decay term, this is possible because of the long phosphorescence lifetime of the triplets and the assumption that the decay due to quenchers in the film is low, a reasonable assumption for low temperatures as the mobility of the excitons towards the quenchers is reduced. As the magnitude of the delayed fluorescence is proportional to the decay rate of the triplets rather than the population it follows that.

$$DF \propto T^2 \qquad \textbf{(Equation 23)}$$

Thus the square root of the DF intensity should be directly proportional to the triplet population, and consequentially the photoinduced absorption signal. When plotted on a logarithmic axis these two lines should therefore appear as parallel. This is shown in figure 3.18 for the data recorded at 225K as the figure shows, the photoinduced absorption data has been smoothed using a 25 point adjacent averaging smoothing algorithm this makes the data considerably more useful over a larger dynamic range, especially when displayed in a logarithmic presentation where the end

of the decay can often appear lost in the noise. The PA data has also been scaled in order to be of the same magnitude at the end of the decay in order to make comparison simpler. A simulation of the prompt fluorescence is also shown; this clearly shows how the end of the prompt fluorescence turning over to the DF as well as how there can be no influence on the DF from the prompt emission after 100ns. The data clearly show a good correlation between the square root of the DF and the photoinduced absorption after 1.1μs. This is strong evidence to back up the assumption that the sole origin of the DF is TTA for this time regime. However, between the end of the prompt fluorescence and 1.1μs there is some difference between the (DF) and the triplet population, there seems to be a fast decaying component of the DF which is not a bimolecular annihilation of the triplets. This is a phenomenon that has been observed previously by Rothe et al. in PF2/6, it was then referred to as DF1 (with the TTA originating DF as DF2) and the source of it remains unclear.

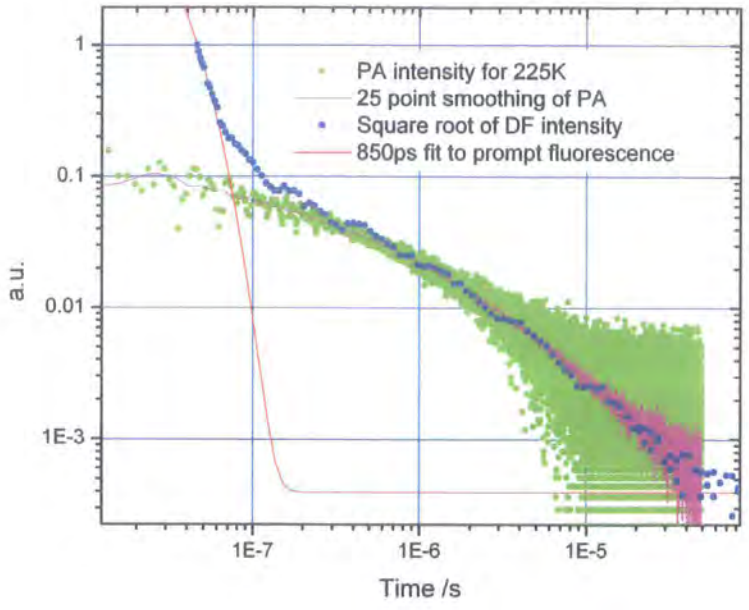

Figure 3.18 Graph showing the similarity between the square root of the delayed fluorescence and the photoinduced absorption. Showing that the DF originates from bimolecular annihilation of the triplets.

If we once again look at the double logarithmic plots of the DF it is possible to see two regions where the decay shows a straight line. This shows that there is a change in the power law that is governing the decay, the turn over in the 160K decay shown in figure 3.16 is from a gradient of -1 to a gradient of -1.7. In order to rationalise this apparent change in mechanism for TTA we must recall the nature of triplet exciton migration as outlined in chapter 2 and mentioned in relation to the solution state experiments. This change in gradient represents a change in the nature of the diffusion of the triplets throughout the film; the change is from the energy dispersive migration from triplets created above the thermal energy level of the material to non dispersive migration within the thermal energy level. This change is seen in all the DF curves, and occurs later as the film is cooled, as would be expected as by cooling the film the level of the thermal energy is reduced, thus there is more

dispersive migration before the equilibrium value of the diffusivity is reached. This explains the time dependant nature of the diffusivity leading to time dependence in the annihilation constant as expected.

In conclusion this chapter has confirmed the origin of the delayed fluorescence in polyspirobifluorene as triplet – triplet annihilation. In isolated chains delayed fluorescence from intrachain annihilation is possible whereas in films annihilation is both inter and intra chain. The turn over from dispersive triplet exciton migration to non dispersive migration below the thermal energy level has also been observed. Importantly we also observed from SSA that the singlets are able to migrate in the solid state whereas they are not able to on isolated chains hence only interchain migration is possible.

Chapter 4

Steady State Photoinduced Absorption

As previously mentioned steady state photoinduced absorption measurements tell us the energy of the triplet – triplet absorption and absorption of other long lived excited states. The photoinduced absorption spectra for a number of conjugated polymers have been measured and the absorptions identified.

PF2/6 - poly(2,7-(9,9-bis(2-ethyl-hexyl)fluorene)) and its Oligomers

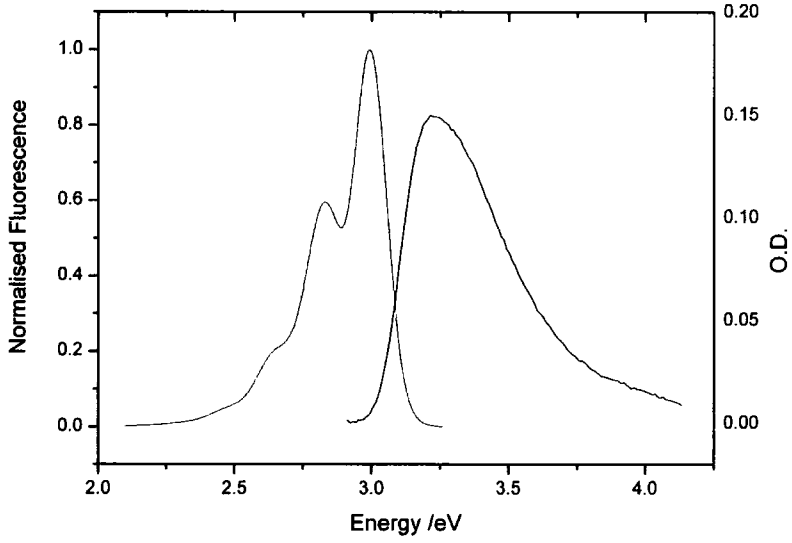

Figure 4.1 Absorption and fluorescence of solution of Pf2/6 in Toluene.

Pf2/6 is a polyfluorene with two 2-ethyl-hexyl groups substituted at the central carbon and is shown in figure 3.1. It has been under study for many years for use in polymer light emitting diodes and much is known about its behaviour. The Pf2/6 and its oligomers were synthesized by Professor U. Scherf at the Max-Planck-Institute for

Polymer Research, Mainz. The absorption and fluorescence spectra of Pf2/6 are shown in figure 4.1. The steady state photoinduced absorption spectrum is shown in figure 4.2 this shows a broad peak at 1.62eV with a steep low energy side and a slowly decaying high energy side, this is consistent with the triplet –triplet absorption spectrum for polyfluorenes and it shows a slight blueshift of 0.1eV compared to the polyspirobifluorene measured previously. This spectrum was measured at room temperature in a degassed toluene solution with a 1cm path length quartz cuvette, the concentration was $1x10^{-5}$ by weight. For this experiment excitation was provided by the 400nm modulated diode laser at a chop rate of 22Hz. The spectrum shows a low noise threshold of about $1x10^{-5}$ which is perfectly adequate as the signal (peaking at $dT/T = 1.04x10^{-3}$) is very strong. However, using a higher modulation frequency might provide better signal to noise ratios.

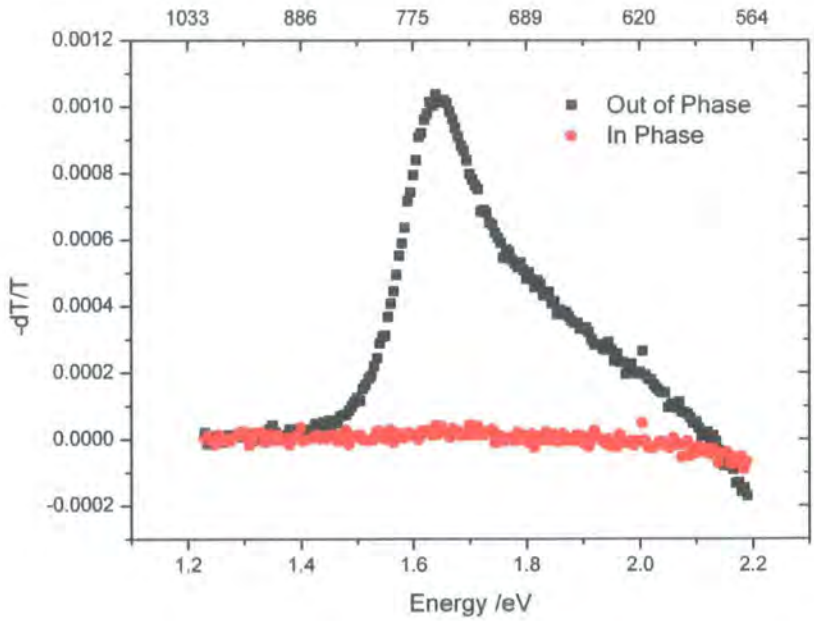

Figure 4.2 Photoinduced absorption spectrum of Pf2/6 solution showing a strong Triplet - Triplet absorption at 1.64eV

One interesting comparison that can be made with PF2/6 is to compare polymers with the same chemical structure but with different chain lengths, this gives

us a way of investigating the effect of the conjugation length on the triplet- triplet absorption. Studies of the effect of conjugation length, both theoretical and experimental on the photophysics of conjugated polymers have been made before extensively in polythiophenes[48, 49], as well as other oligomers of conjugated polymers[50-52]. However, most studies have investigated the UV/vis ground state absorption and the position of the first triplet state, the variation in the T_1-T_n energy gap has only been extensively investigated for polythiophenes and poly(para-phenylenevinylenes).

The variation of both the ground state absorption and the Triplet – Triplet absorption with oligomer length can be used to investigate the spatial extent of the excitons on the chain. For example if we consider a scenario where the exciton has a maximum size of 10 oligomer repeat units it is logical to assume that if the exciton sits on a polymer chain that is 100 units long it will be no different than if it sat on a chain only 20 units long. However if the exciton took up say 25 repeat units then the exciton on the shorter oligomer would be altered, effectively constrained by the polymer itself and as a result the electron and hole become closer together increasing the Coulomb interaction and raising the energy of the exciton. Thus the absorption peak may shift to a higher energy, although there remains the possibility that both T_1 and T_n would change. However, there are two factors that could be controlling the exciton size; the first is the intrinsic binding energy of the exciton itself, a relatively simple concept if we consider the exciton as an electron orbiting a hole in hydrogen like manner, the radius of the orbit is determined by the binding energy of the exciton. The other constraint on the exciton size is the effective conjugation length of the polymer itself; this is the length of polymer chain that contains conjugation unbroken

by defects, ring twists and other structural anomalies within which the exciton must remain.

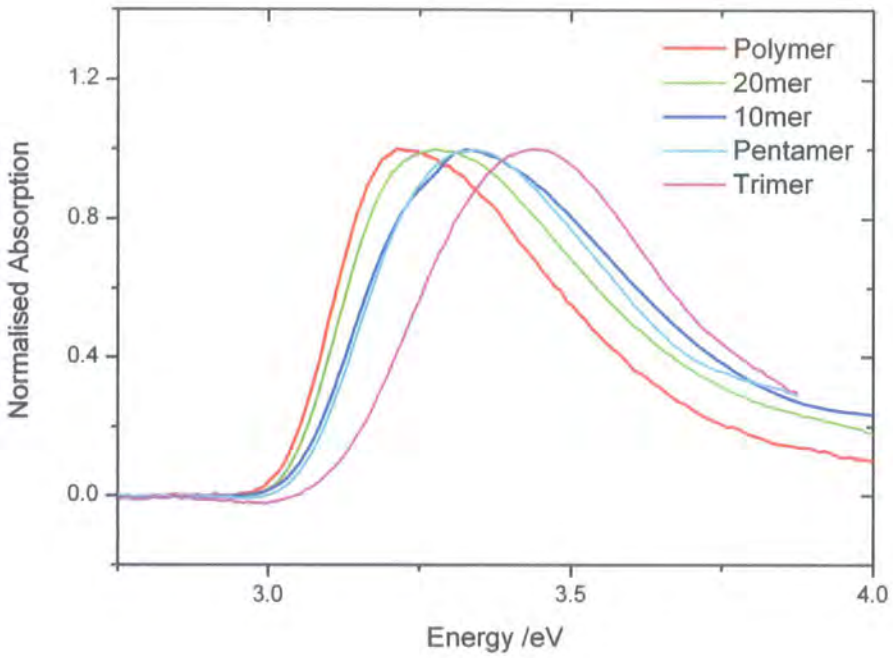

Figure 4.3 Variation of the Absorption spectrum of Pf2/6 solutions with chain length.

Figure 4.3 shows a comparison between the ground state absorption spectra of PF2/6 polymer and oligomers of PF2/6 that are 3, 5, 10 and 20 repeat units long. The polydispersity of the 10 unit oligomer, 20 unit oligomer and polymer were 2.5, 2.3 and 2.0 respectively whereas the pentamer and trimer were synthesized with only a fixed number of repeat units. The data has been normalised to the peak of the fluorescence to allow easier comparison. The variation in conjugation length between the oligomers has a clear effect on the position of the absorption. The absorption moves to higher energy as the conjugation length shortens, an exception seems to be with the tenmer and pentamer which have almost identical absorption spectra, this

could be an effect of the synthesis, as the trimer and pentamer were synthesised with a pyridine ring terminating one end of the chain rather than phenyl rings. Figure 4.5 shows that these data approximately obey a linear relationship with 1/n with a gradient of 0.66. This is consistent with other data in the literature[52] for the oligoenes, oligothiophenes and OPVs.

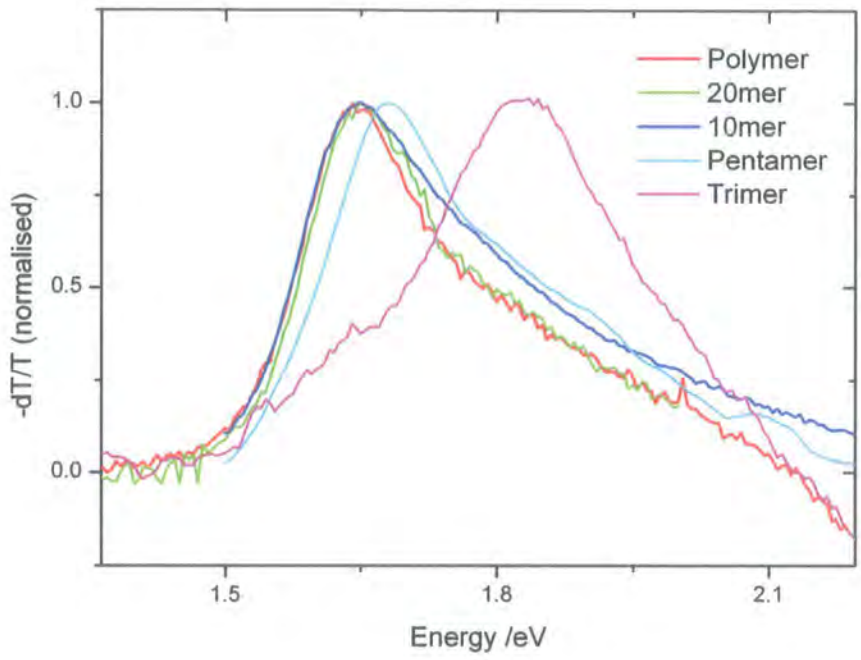

Figure 4.4 Normalised Triplet - Triplet absorption spectra for oligomers of Pf2/6 showing a clear deviation from the polymer like behaviour for chains shorter than 10 units long.

If we now look at the Triplet – Triplet absorption spectra in figure 4.4 a different dependence is seen, the polymer, 20mer and 10mer have the same photoinduced absorption whereas the variation with conjugation length seen in the ground state absorption is only seen in the shortest oligomers. The data for the pentamer and trimer have been smoothed with a 15 point adjacent averaging algorithm, this was necessary because they have very low signal magnitudes due to the reduced ground state absorption of the 400nm pump laser. It is also interesting to note that the trimer spectrum has a slight shoulder at about 1.65eV. There are two

possibilities for this the first is contamination with longer polymer chains which could produce the additional photoinduced absorption. The other possibility is that the trimer has become aggregated in the solution producing a state with increased conjugation, this would be similar to the behaviour of PFO in solution which is described in more detail in the second half of this chapter.

The onset of absorption of the oligomers was also measured and is plotted in figure 4.5 against n, the length of the polymer, by assuming the linear dependence of the absorption with 1/n is true it is possible to use this data to calculate the effective conjugation length for the singlet exciton, most likely determined by the frequency of structural defects on the polymer backbone which confines the singlet. This is done by fitting the data for the oligomers, in which we must assume that the majority of the chains do not contain structural defects, to the equation shown on the graph and from the intersect of this fit with the energy of the onset of absorption of the polymer itself we can estimate the effective conjugation length of the polymer. From this we can see that the effective conjugation length is considerably shorter than the length of the polymer chain itself, some 25-30 units in comparison to the 260 unit length expected from the mean molecular weight of the polymer. This in turn suggests that the mean separation of the structural defects is between 25 and 30 units.

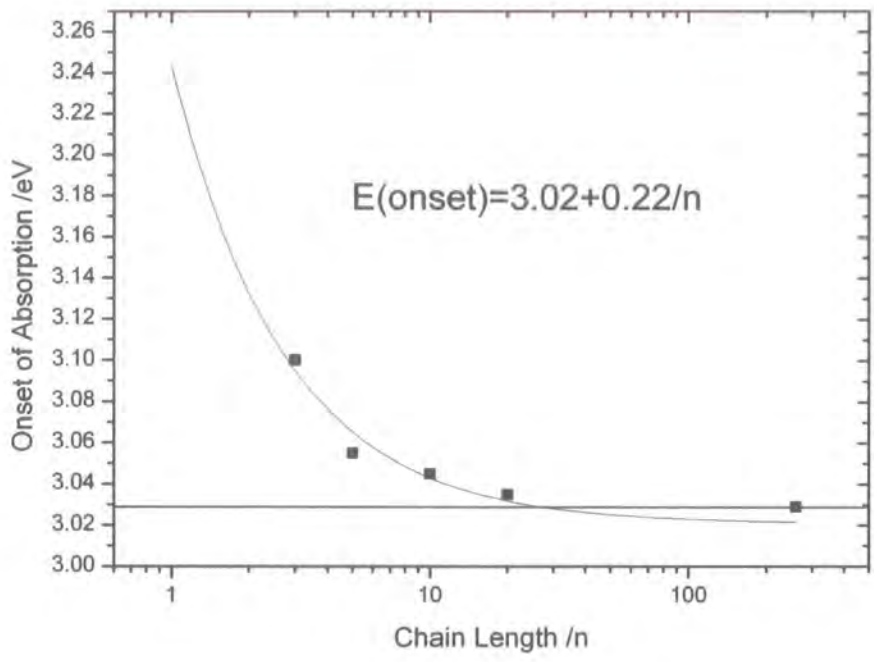

Figure 4.5 The onset of ground state absorption against chain length, fitting the oligomer data allows the calculation of the effective conjugation length of the polymer.

In figure 4.6 positions of the absorptions have been plotted against 1/n and the difference between the behaviour of the absorption and photoinduced absorption is clear. These plots provide a clear way of testing the contributing factors to the exciton size; if the exciton were being confined purely by conjugation breaks in the polymer than one would expect to see the same dependence on length for the absorption of both the triplet and the ground state. However as this is not observed, it leads us to conclude that the triplet exciton size is defined more intrinsically, this can only be concluded for the triplet because no turn over is seen for the ground state absorption dependence indicating that the singlet can occupy a considerably larger conjugation length given a long chain.

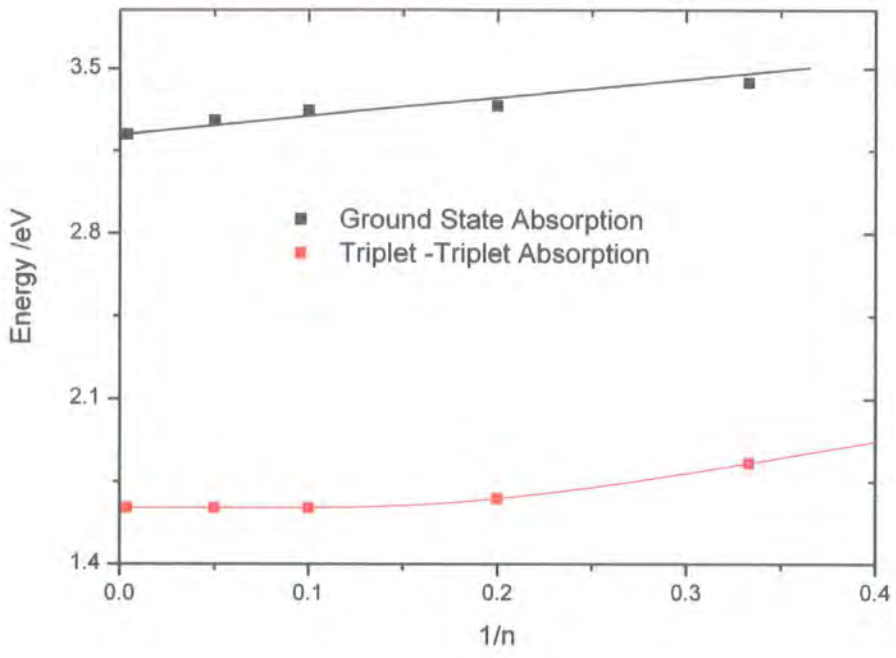

Figure 4.6 Variation of Ground state and Triplet -Triplet absorptions with inverse chain length

As previously mentioned the ground state absorption dependence on the inverse conjugation length follows approximately a straight line and this can be extended to estimate the absorption for the monomer to be 3.9 ± 0.1 eV. The fit line for the triplet exciton dependence is from equation 24.

$$E(n) = E_{\infty} + (E_1 - E_{\infty})\exp[-a(n-1)] \qquad \textbf{(Equation 24)}$$

The derivation[53, 54] of this equation assumes a clearly defined energy gap for the polymer E_{∞}, the monomer E_1, the length of the oligomer n and a fitting factor a which expresses the sharpness of the turn over from the exciton energy being defined intrinsically (large n) or by the constraints of the conjugation length (small n). From this turn over point we can estimate the triplet exciton size to be approximately 5 repeat units long. The fitting also gives an estimate for the energy of the Triplet – Triplet absorption for the monomer as 2.5 ± 0.1 eV. Unfortunately this can not be verified as neither the 400nm diode laser nor the Ar+ laser used as the pump can provide excitation of the monomer because the ground state absorption spectrum is shifted to too high an energy.

The variation of the ground state absorption with effective conjugation length is similar to that observed previously in polythiophenes the linear relationship with 1/n was once again found. However, in polythiophenes the $T_1 \rightarrow T_n$ absorption appeared to act much more like the singlet absorption with no deviation from a linear dependence with 1/n. This was attributed to the highest triplet exciton being as delocalised as the singlet state. However the lowest triplet state as measured by pulse radiolysis energy transfer does show a deviation from the linear dependence with 1/n at between 4 and 6 repeat units, this was attributed to electron delocalisation in the triplet state. Further confinement of the triplet exciton to 1 or 2 repeat units is expected from theoretical models based on single particle theories[55] and ODMR measurements[56, 57]; this theory is also supported by evidence from experiments with both fluorene[58] based copolymers and carbazole-oxadiazole based copolymers[59] where the triplet can become confined by making the polymerisation at different positions on the phenyl ring, experiments of this type suggested that the triplet exciton was confined even further to as few as two phenyl rings. The results for polyspirobifluorene seem to allow for a middle ground, with the triplet exciton being less delocalised than in the case for polythiophenes, but more delocalised than in carbazole based polymers.

PFO – Poly 9,9 - dioctylfluorene; solvent effects leading to aggregation.

PFO is one of the simplest polyfluorenes, with two eight carbon alkyl chains substituted at the central carbon of the fluorene unit shown in figure 3.1. However, the simplicity of the substitution leaves PFO with some unusual properties[60, 61], most polyfluorenes in the solid state form a stable glassy phase which is resistant to most polymer processing techniques. However, PFO films exhibit some interesting features when they have undergone annealing processes, thermal cycling (even below the glass transition temperature) or exposure to certain solvent vapours. Solutions are also susceptible to changes when thermally cycled for example during degassing or when poor solvents such as methylcyclohexane are used. The most noticeable is a change in the absorption spectrum; additional features appear which are consistent with an additional spectrum with well defined vibronic character being superimposed over the original absorption spectrum. A redshift in the fluorescence spectrum of 0.1eV is also observed. It appears that there is some kind of phase change in the material during the treatments thus creating a new absorption spectrum which is superimposed on the absorption spectrum of the remaining glassy-phase PFO; this is known as the β-phase of PFO.

The β-phase has been extensively studied in recant years[60-62] it is most intuitive to assign changes due to solvent effects to some form of aggregation with interchain effects becoming important. However in the β-phase of PFO there is no indication of broad excimer like emission often characteristic of interchain

interactions or reduction in quantum yield like that observed[63] in MeLPPP. In this ladder type polymer it is believed that aggregates form and the excitiations can efficiently transfer from the bulk to the aggregated states which decay by a broad yellowish emission. The β-phase properties are in fact more consistent with the formation of a phase with extended conjugation. Comparison with the fully planar MeLPPP has yielded two possibilities for the cause of this, either the PFO is forced more planar by interchain interactions within the β-phase or the excitations are in fact located on interchain orbitals extending throughout the entirety of each of the β-phase segments.

As well as changes in the ground state absorption spectrum aggregation causes changes in the photoinduced absorption, indicating that the morphology affects the triplet state as well as the singlet. In this chapter I have further investigated the nature of the changes to the photoinduced absorption and their causes. The PFO used in the study was synthesized in the Department of Chemistry, University of Durham, by Dr Batsanov.

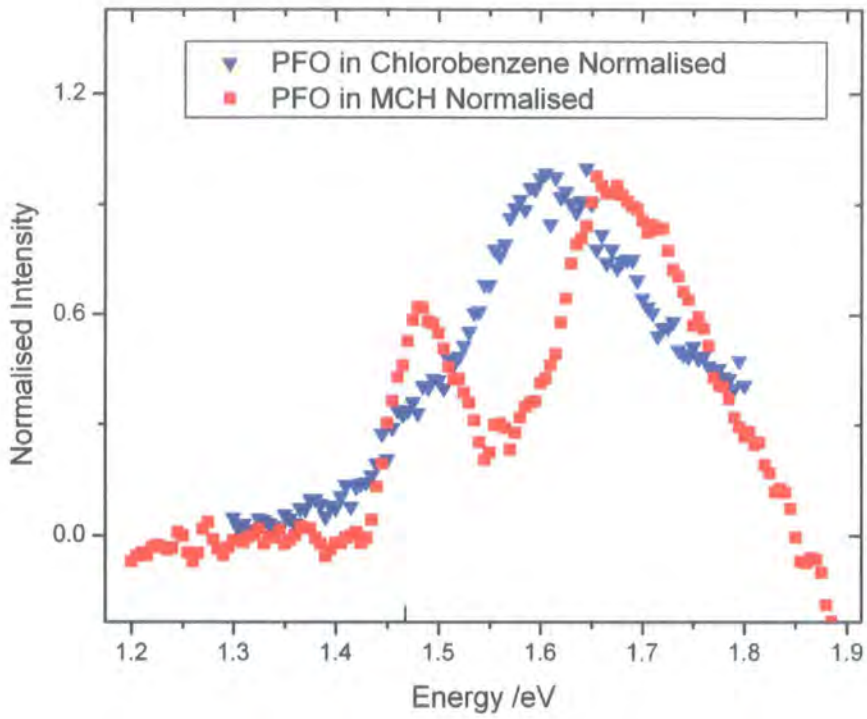

Figure 4.7 Normalised photoinduced absorption spectra for PFO in Chlorobenzene and MCH.

Absorption and fluorescence spectra show similar results to the other polyfluorenes for the polymer dissolved in toluene solution. Figure 4.6 shows the photoinduced absorption spectrum of degassed chlorobenzene solution at room temperature, the data was taken using the tungsten filament lamp as the probe beam and excitation was provided by the 400nm modulated diode laser with a modulation frequency of 72Hz the spectrum shows a peak at 1.60eV which has a width of 0.23eV FWHM this is attributed to the triplet – triplet absorption and is consistent with spectra recorded for other polyfluorenes, this is in no way surprising. However when PFO is dissolved in MCH there is a significant change in the photoinduced absorption spectrum, as the red line in figure 4.6 shows, the triplet exciton peak splits into two, one transition at 1.64eV and another smaller one at 1.47eV; the decreasing signal above 1.8eV is the tail of the fluorescence spectrum of the polymer. The peak at

1.64eV is once again attributed to the triplet exciton of the dissolved polymer; the 0.04eV blue shift is due to the lower solvent polarity of MCH in comparison to toluene. The lower energy peak is attributed to the triplet exciton of PFO chains in the β-phase. If we look carefully again at the PIA spectrum in chlorobenzene there is a small knee on the low energy side of the triplet - triplet absorption peak which indicates that there a small number of chains in the β-phase even in good solvents, this feature is similar in nature to that observed in the three unit oligomer of PF2/6 previously, suggesting that the shorter chains are more likely to form aggregates.

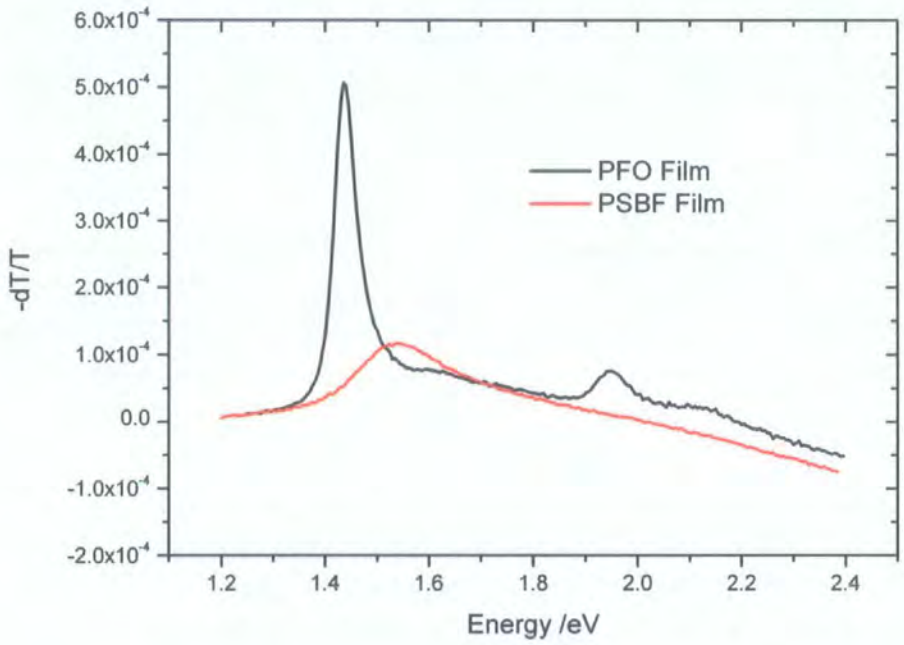

Figure 4.8 Comparison of the in phase components of PA spectrum for PSBF and PFO films.

We can take the observations of PFO solutions further by looking at PFO in the solid state, solutions were drop cast onto quartz substrates from a 10mg/ml solution in MCH. PIA spectra were obtained with the sample at 77K in a liquid nitrogen cryostat. The spectra obtained show a surprising result when compared to other polyfluorenes like PSBF these are shown in figure 4.7. The spectrum features a

large sharp absorption at 1.42eV and a smaller peak at 1.95eV along with these two weak shoulders are observed at 1.64eV and 2.11eV as well as the negative going signal from the photoluminescence at high energies. The similarities with the MCH solution spectrum allow us to assign the 1.42eV and 1.64eV to the triplet – triplet absorption of the β-phase and 'normal' solution state exciton of PFO. Assignment of the higher energy features is more complex; Cadby and Wohlgenannt *et al*[60] have attributed the 1.95eV feature to transitions of polarons and indeed using an FTIR photoinduced absorption spectrometer setup they are able to observe another polaron like absorption below 0.5eV. However, having recorded the spectra at two different pump beam modulation frequencies, the two large peaks have the same relative intensities whether recorded at a chop rate of 720Hz or 72Hz although the magnitude of the signals at 720Hz is approximately 1/10 of that observed at 72Hz. This confirms that the two peaks obey the same decay kinetics; with this in mind the 1.95eV feature is attributed to a higher absorption from the first triplet state (T_1-T_m) where the 1.42eV feature is the original (T_1-T_n) absorption. This would naturally have the same kinetics as the 'normal' triplet excited state as it is the kinetics of the initial state that are measured in this way. The shoulder at 2.11eV can be understood in the same way, this is a higher transition (T_1-T_m) of the amorphous triplet, this conclusion is supported by the fact that the splitting of the two higher transitions is approximately the same as the splitting of the two (T_1-T_n) transitions. It is also possible to just see the higher triplet transition (T_1-T_m) on the PSBF. This is noticeable where the spectrum turns over to become the fluorescence and an additional shoulder is just visible. It is an interesting question to ask why this transition was not visible in solution state experiments. The answer is simple, we were unable to see the higher transition of the amorphous triplet because they were masked by the high

luminescence of the solutions as they are within the edge of the polymer fluorescence; however the films have sufficiently quenched luminescence that the higher transition of the amorphous polymer is visible.

These results have shown that the β-phase of PFO can form not only in the solid state, but in poor solvents. The formation of the β-phase shifts the T_1-T_n absorption to lower energy suggesting that there are segments of extended conjugation. An additional higher T_1-T_m transition is also observed for both the β-phase and the amorphous triplet for films containing the β-phase. The amorphous triplet was also observed in both the β-phase films and solutions in poor solvents, so even though a large number of β-phase segments are formed, not all polymer chains are in the segments.

Chapter 5

Guest – Host Energy Back-transfer in a Phosphorescent Dye doped Polymer System.

As outlined previously one of the current problems in PLEDs is loss of efficiency from the triplet state. As we know charge recombination in devices results in a singlet – triplet ratio of up to 25%:75% which results in a considerable reduction in the number of emissive states[18, 19]. The best way to circumvent this problem is to harvest the triplet states for light output, thus allowing a considerably higher proportion of the excited states to contribute to the overall device efficiency. If we consider the nature of triplet generation after photo creation of singlets, intersystem crossing from the singlet state we remember that the rate of intersystem crossing is considerably enhanced by the presence of a heavy atom due to the spin orbit coupling, consequently the rate of phosphorescence is enhanced as well. With these two considerations in mind it is possible to dope the polymer in a PLED with a phosphorescent heavy metal complex; giving a large increase in device efficiency[8, 64-69].

The method by which the phosphorescent complex in an electroluminescent device can be excited is by either one or both of the following ways; firstly energy transfers from the conjugated polymer host material, by resonant forster energy transfer. Or by acting as preferential electron trapping sites which allow charge recombination on the complex[70, 71]. In photoexcitation experiments the complex can

once again be excited by energy transfer from the polymer host or by directly exciting in the absorption band of the complex itself. The latter method allows us to more easily understand the processes involved in the decay of the triplets on the complex and any energy transfer processes that depopulate the complex. The only problem that can arise is due to the relative strengths of the absorption bands of the polymer and complex, in a doped system as there are relatively few molecules of complex compared to the polymer the absorption into the complex is negligible compared with that of the polymer therefore, in order to carry out experiments of this type the blend must be excited away from the absorption band of the polymer with a relatively large laser dose in order to create enough triplets on the dopant.

However, there is one problem with phosphorescent dye doped devices which lies in the triplet level of the polymer; if the triplet level of the polymer is lower than that of the phosphorescent complex then triplet energy transfer can take place from the complex back to the polymer, quenching the phosphorescence of the complex. The low triplet energy of most of the conjugated polymers suitable for PLED applications makes this a major stumbling block for the design of electrophosphorescent devices which emit in the blue and green regions of the spectrum, new polymers are being developed to overcome this barrier, one commonly used polymer polyvinylcarbazole (PVK) has a suitable triplet energy but unfortunately there is a hole injection barrier of approximately 1eV resulting in devices with low luminence and high onset voltage. Other such suitable polymers are the newly developed carbazole-oxadiazole based copolymers previously mentioned[59]. However, there is another solution; as outlined previously triplet energy transfer occurs by the Dexter process, requiring overlap of the electronic orbitals of the guest

and host. It is now an elementary step to imagine reducing the orbital overlap by separating the polymer chains from the complexes by the addition of bulky side groups on the complex which physically prevent close contact between the chains and the complex[24], similarly the same effect could be achieved by using a polymer with bulky side group. For example it is possible to envisage the conjugated part of the complex surrounded by a shell of unconjugated alkyl groups to prevent energy transfer.

In some cases the cycling of energy from the singlet to the triplet via the complex on the polymer can be advantageous, as it provides a way of enhancing the triplet population on the polymer. This method has been used with Benzil as the triplet enhancer by Rothe et al to aid investigation into polymer triplet energy transfer[72].

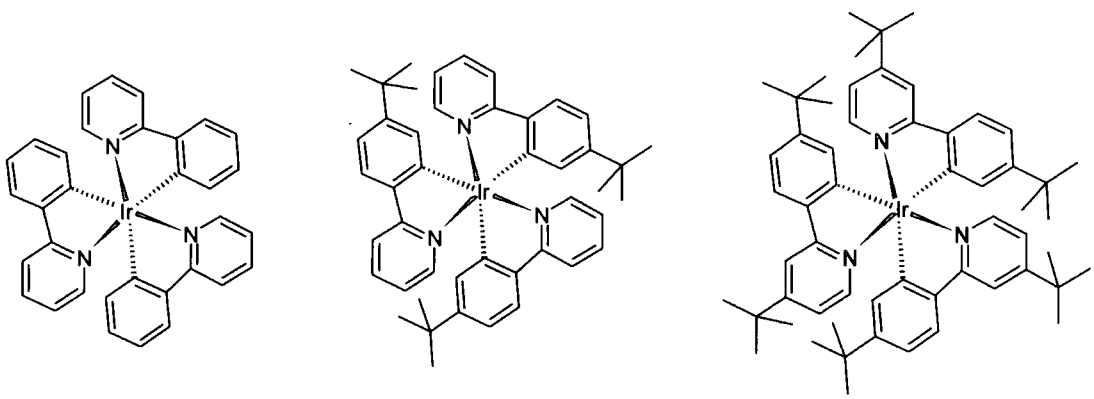

Figure 5.1 The Iridium(III) complex dopants used in the study.

The efficiency of a device in which there is triplet back transfer is directly affected by the rate of the energy transfer; this can be measured directly using time resolved photoinduced absorption to measure the build up of triplet states as they

return to the polymer host. Experiments have been carried in this way out to test the method of reducing the back transfer and hence increasing the efficiency of the device. Rates of back transfer were measured for polyspirobifluorene doped with $Ir(PPY)_3$ and two derivatives: $Ir(BuPPY)_3$ and $Ir(Bu_2PPY)_3$ the structures are shown in figure 5.1. All the complexes used in the study were kindly provided by Dr A. Beeby at the department of Chemistry, The University of Durham.

As with all tris-chelates the complexes are able to form in both the *fac* (facial) and *mer* (meridianal) isomers, however, the *fac* isomer shows considerably higher luminescence quantum yield[73], and indeed the *mer* isomer is known to rearrange to the *fac* under UV irradiation. For all the complexes in this study the *fac* isomer has been used. This use of the *fac* isomer has an interesting implication when the phenol or pyridine ring on the ligand has an isobutyl substitution at one of the carbons; if both are substituted the effect is to form a shell around the complex with the butyl groups. If only one ring is substituted the effect is a shell over only one half of the complex. This hemisphere effect gives us the shielding effect required to reduce the energy transfer.

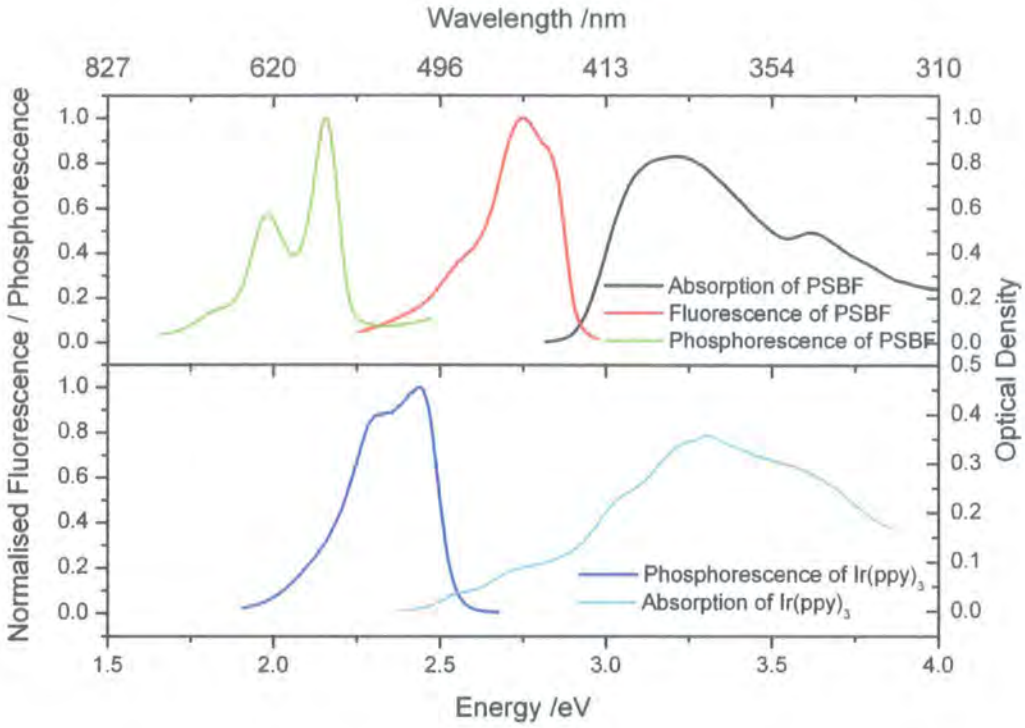

Figure 5.2 Absorption fluorescence and phosphorescence of PSBF films (top), Absorption and phosphorescence of $Ir(ppy)_3$ in zeonex films.

In order to ascertain the energy levels of the system absorption, fluorescence and phosphorescence spectra were obtained for PSBF and the absorption and phosphorescence were obtained for the complexes, these are shown in figure 5.2. Theoretical calculations have been carried out by *Hay*[74] which indicate that the feature in the absorption spectrum of $Ir(ppy)_3$ at 494nm is the triplet MLCT state and slightly higher in energy is the singlet MLCT state which rapidly undergoes intersystem crossing to the lower energy triplet due to the large heavy atom effect[75]. An energy level diagram for the system is shown in figure 5.3.

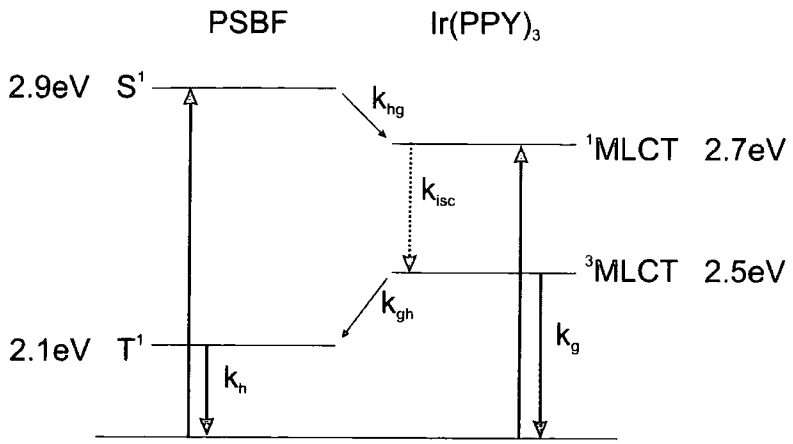

Figure 5.3 Energy level diagram of the polymer - complex system. The thick black lines represent excitation and emission and the thinner lines represent radiationless energy transfers between the states

The emission from the Iridium complex at 510nm (2.43eV) remains the same for all the complexes, indicating that the isobutyl substitutions have no effect on the ^{3}MLCT state allowing more simple comparisons to be drawn. This is as expected as the isobutyl groups can take no part in the conjugation and hence would not be expected to influence the $d_2 - \pi^*$ ^{3}MLCT transition, although it is conceivable that there could be an increase in electron density on the rings from the electron donating isobutyl groups[76], this effect is clearly to small to have an influence. Steady state photoinduced absorption spectra have been obtained for $Ir(PPY)_3$ and PSBF and are shown in figure 5.4 the spectrum for PSBF has been explained previously. The $Ir(PPY)_3$ spectrum shows a peak at 400nm attributed to the triplet MLCT state and the other feature at 450nm is attributed to the photobleaching of the ground state absorption, these features are consistent with reported spectra for this and other Ir(III) complexes[77]. As the triplet-triplet absorptions of the two components are well separated with no overlap it is possible to probe the photoinduced absorption of the PSBF without it being affected by any change in the intensity of the PA of the complex.

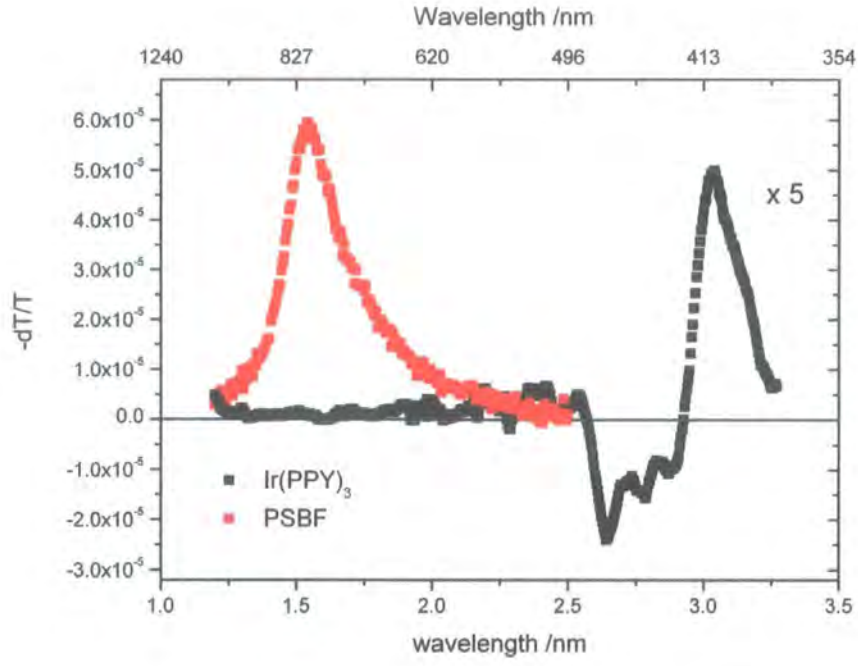

Figure 5.4 Photoinduced absorption spectra of PSBF film and $Ir(ppy)_3$ zeonex film, the $Ir(ppy)_3$ has been scaled by a factor of 5 for ease of comparison. Only the out of phase componants are shown as the in phase componant is dominated by the strong phosphorescence from the complex.

Films of PSBF containing approximately 7% by weight of the Ir(III) complexes, the dopant level is only approximately 7% because the level was varied from complex to complex to ensure that the same concentration of Iridium atoms was present in all the films. The films were spun at 1200rpm onto sapphire substrates from either toluene or in the case of the unsubstituted $Ir(PPY)_3$ chlorobenzene. Steady state emission spectra after excitation at 355nm were recorded and are shown in figure 5.5 alongside a spectrum for undoped PSBF and $Ir(PPY)_3$. It is important to note that although excitation at 355nm is within the absorption bands of both the polymer and the complex the absorption of the complex in the films is negligible compared to the polymer so much so that it is not detected by the spectrophotometer. Thus all the excitations that subsequently appear on the complexes arrive via the polymer, which is a clear indication that förster transfer is strong in this case. The emission of the films already gives a clue as to the relative rates of energy transfer. The most

substituted ligand shows an increase in the size of the peak at 510nm originating from the $Ir(xPPY)_3$, showing that there are either more triplets created on the complex or that they are less able to transfer away before undergoing a radiative decay. It is also important to note the magnitude of the PSBF emission peaks, not only are they all considerably quenched in comparison to an undoped film, but the doubly substituted film has a larger PSBF peak. This could be an indication that the substitution is affecting the rate of Forster transfer from the PSBF to the complex.

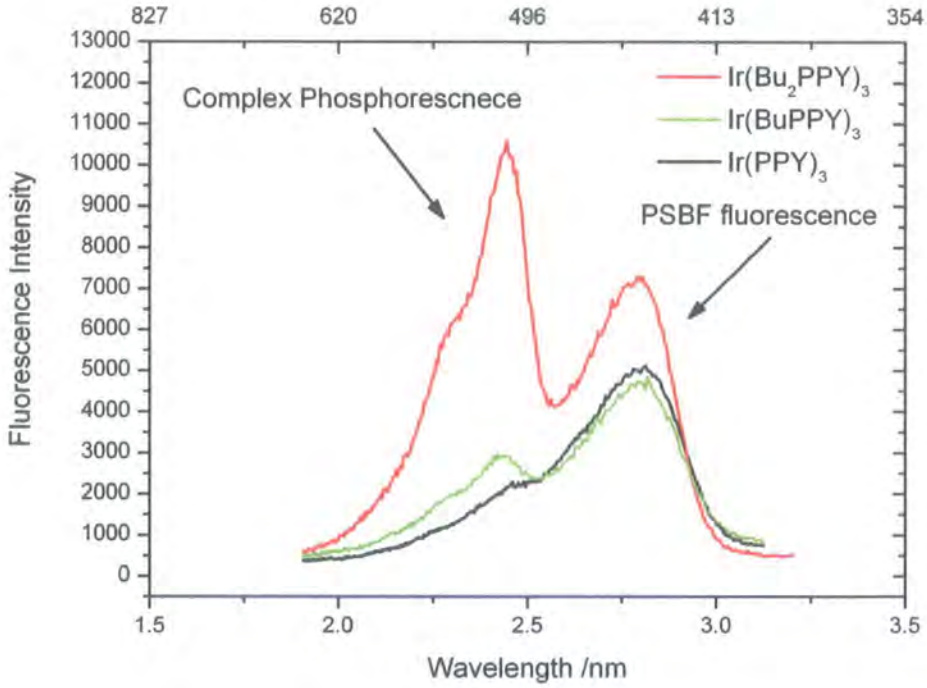

Figure 5.5 Steady state emission of films of PSBF blended with the various Ir(III) complexes, these data are not normalised and it is important to note that the magnitude of the PSBF fluorescence peak is approximately 3 orders of magnitude smaller than for an undoped film.

Time resolved photoinduced absorption measurements were then made on the films at 80K. In this experiment the triplet population of the PSBF was monitored after direct excitation of the complex. This was done using a dye laser containing a solution of Coumarine 500, which lases at 495±5nm providing excitation directly into

the MLCT bands of the complex. Crucially this is outside the absorption spectrum of PSBF thus ensuring that any triplets that subsequently appear on the polymer have undergone an energy transfer from the complex. The probe beam was a 785nm diode laser which was detected by a 2GHz amplifier and recorded on the oscilloscope as described in more detail in the experimental section. It was necessary to use considerable laser power to excite the complex due to the low absorption and low concentration of the complex in the film; indeed the absorption spectrum of the doped films does not show any absorption for the complexes at all, although the emission spectra more than verify its presence. The build in for the PSBF triplets after excitation of the complex are shown in figure 5.6. These have been smoothed and fitted to a single exponential build in function to give a build time. The build in times show a slower build in as the isobutyl groups are added.

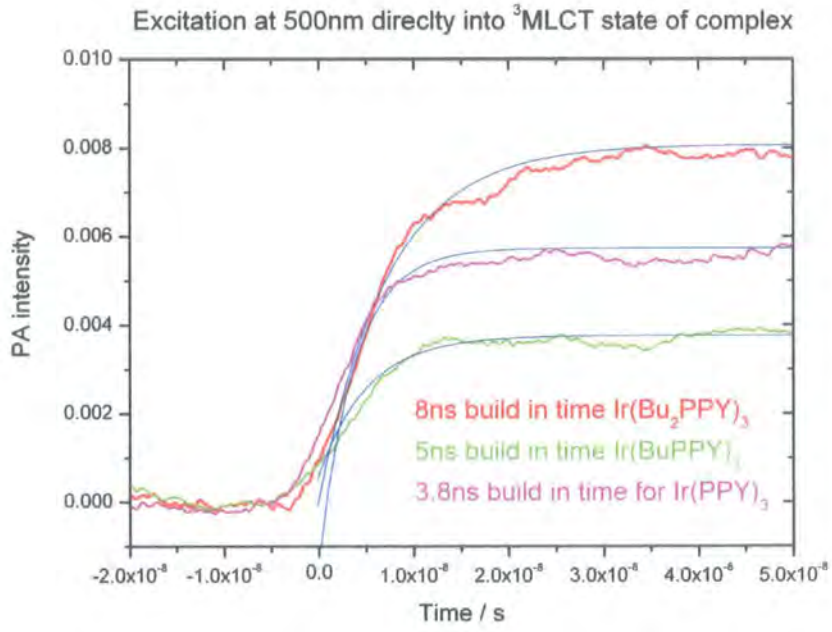

Figure 5.6 Build in of triplets on PSBF following excitation of the complex at 500nm. The build in of triplets in a film of PSBF following excitation of the PSBF itself is faster than the time resolution of the experiment.

The slowing of the build in clearly suggests that the protective shell of the isobutyl groups on the ligands is slowing the rate of triplet energy transfer to the polymer (on the energy level diagram this is marked as k_{gh}). The reasoning behind this is relatively simple; the energy is transferred through the Dexter mechanism thus requiring overlap of the donor and acceptor orbitals. The wavefunction of the orbitals decays exponentially; moving the donor away from the acceptor reduces the orbital overlap considerably thus the energy transfer is less efficient. This rate of energy transfer by the Dexter process is governed by the equation[78].

$$k_{da} = k_d \exp\left[\gamma_{da}\left(1-\frac{R}{R_0}\right)\right] \qquad \textbf{(Equation 24)}$$

With k_{da} the rate of energy transfer form donor to acceptor, k_d the lifetime of the donor, $\gamma_{da}=2R_0/L$ where L is a distance characterising the interaction range known as the Bohr radius; R_0 the critical radius for energy transfer and R the separation of donor and acceptor.

If we take the most simple case of the isobutyl groups on the $Ir(Bu_2PPY)_3$ forming a shell around the excited complex which inhibits the energy transfer to the polymer using equation 24 it is possible to estimate the critical radius for energy transfer R_0; we calculate this to be 1.2nm. This is however a lower bound as in using equation 24 we have assumed that the complex and the polymer are solid objects in contact with one another when in reality there may be free space between them.

It is advantageous at this point to consider a kinetic scheme for the blend, in the first instance following excitation of the polymer host. We consider all of the excitations to form on the polymer and undergo energy transfer, this is possible because of the relative strengths of the absorption bands of the polymer and complex, in this scenario we must consider both energy transfer to the complex and back

transfer away. In the equations below the 'h' subscript denotes the host polymer and the 'g' the guest complex.

$$\frac{dS_h}{dt} = G - (k_{hg} + k_r + k_{nr})S_h$$

$$\frac{dN_g}{dt} = k_{hg}S_h - k_{gh}N_g - k_g N_g$$

$$\frac{dN_g}{dt} = k_{gh}(C\exp(-k_h t)) - (k_{hg} + k_g)N_g$$

in this scheme, S_h denotes the number of singlets on the host, N_g the number of excitations on the dopant (strictly the excitations are Förster transferred as singlets and then undergo intersystem crossing to triplets, from which they transfer back to the host.) k_r, k_{nr}, and k_{hg} are the radiative and non radiative decay rates for the polymer and the rate of Förster transfer to the complex respectively; k_{gh} and k_g are the rates guest host triplet back transfer and the radiative decay rate for the complex.

In the simplified case of the photoinduced absorption experiments carried out we can neglect the effect of the energy transfer to the complex as excitation was carried out exclusively in the absorption band of the complex, using the same notation as above this simplifies the kinetic scheme as follows.

$$\frac{dN_g}{dt} = G - (k_{gh} + k_g)N_g$$

$$\frac{dT_h}{dt} = k_{gh}N_g$$

In this case T_h is the number of triplets on the host polymer which as we can see is only dependant on the rate of Dexter transfer from equation 24 and the number of excitations on the complex.

It might be expected that the overall magnitudes of the photoinduced absorption peaks would be related to the efficiency of the transfer; the blend with the most efficient energy transfer would give the highest number of polymer triplets. This was not observed. However, this observation does not really contradict the findings from the build in times as there are many more factors to include when considering the number of triplets produced, these include the relative magnitude of the absorption of the individual complexes, the film thickness as well as the number of iridium atoms in the films.

In summary we can draw the conclusion that the rate of triplet back transfer from an excited dopant with triplet energy above that of the host can be manipulated by adding bulky side groups to the dopant to change the spatial proximity of the dopant to the host polymer. This in turn reduces the rate of Dexter energy transfer to between the dopant and the host polymer. This will in turn increase the efficiency of electrophosphorescent devices where the triplet level of the phosphorescent dye is higher than the triplet level of the host polymer.

Conclusions

As outlined many times previously there is much importance attached to the triplet stated in conjugated polymers and in particular the polyfluorenes. The investigations carried out for this thesis have given an insight into the nature of the build in and decay of triplets in polyfluorenes, there are a number of firm conclusions that can be drawn from the results.

Time resolved photoinduced absorption and gated emission studies have been made on pristine and blended films as well as dilute solutions of Polyspirobifluorene (PSBF). Upon photoexcitation in solution triplets are formed on isolated chains of PSBF by intersystem crossing and the rate of formation of triplets reflects the rate of decay of the singlet exciton, thus proving that the nature of triplet production is via intersystem crossing.

If triplet excitons are formed on the individual chains in sufficient density then the excitons are able to travel along the chains and take part in intrachain triplet – triplet annihilation reactions which give rise to delayed fluorescence. However, it appears that the singlet excitons are unable to travel along the chains as there is no evidence of singlet-singlet annihilation even though a large number of singlets are created on each chain.

In the solid state, films of PSBF were investigated; annihilation reactions also occur however the close proximity of the polymer chains allows for both intra-chain and inter-chain annihilation to occur. It has been shown that these annihilation

reactions are the origin of delayed fluorescence in films of PSBF. This is consistent with the delayed fluorescence observed in other polyfluorenes. Unlike in solution state experiments singlet-singlet annihilation was observed in addition to triplet-triplet annihilation, and this in comparison to the solution state work suggests that the singlets are only mobile between the chains rather than along them.

The triplet state in conjugated polymers can also be populated by energy transfer, we have shown that in blended films of PSBF and $Ir(PPY)_3$ and similar complexes energy transfer from an organic phosphor can form triplet excitons on PSBF chains. This gives a slower build in of the triplets on the polymer than direct photoexcitation and intersystem crossing we have demonstrated that as triplet energy transfer is by the Dexter transfer mechanism the rate of energy transfer can be manipulated easily. The addition of bulky groups which do not change the photophysics of the complex, in this case isobutyl groups, can slow down the energy transfer by separating the dopant from the polymer chain, thus reducing the overlap of the orbitals necessary for Dexter transfer. Reducing the rate of triplet back transfer in a blended polymer and phosphorescent dopant system reduces the number of triplet excitons lost to the weakly emissive polymer triplet state thus increasing the phosphorescence of the dopant.

An investigation into the steady state photoinduced absorptions of some other polyfluorene derivatives has lead to some interesting conclusions. Firstly the variation of the ground state and triplet – triplet absorption of oligomers of PF2/6 has shown that triplet exciton occupies only a short, approximately 5 unit, conjugated segment of the chain, whereas the singlet occupies a considerably larger conjugation length,

approximately 25 units and is most likely constrained by defects in the structure of the same separation.

Steady state photoinduced absorption spectra of films and solutions of PFO have shown that in poor solvents and an alternative morphology of the polymer can form known as the β-phase. In poor solvents this gives rise to a shift in the photoinduced absorption spectrum which is observed along with the features for the amorphous polymer. However, in films of the β-phase not only is the shift observed, but the reduced luminescence compared to the solution allows a higher absorption of the triplet to be resolved, for both the β-phase peak and the amorphous triplet.

These investigations into the triplets of polyfluorenes and polyspirobifluorenes have yielded results which will help to further the understanding of triplets in conjugated polymers. This understanding will ultimately be useful in improving the efficiency electroluminescent devices based on emission from conjugated polymers and blends of conjugated polymers and organic phosphors.

Publications

The publications listed below were published as a result of work contained in this thesis.

'Triplet Build in and Decay in Isolated Polyspirobifluorene chains in Dilute Solution' S. King, C. Rothe, and A. P. Monkman, Journal of Chemical Physics, (in press) (2004).

'The Triplet Exciton State and Related Phenomena in the β-phase of Poly(9,9-dioctyl)fluorene' C. Rothe, S. King, F. Dias and A. P. Monkman, Physical Review B, (in press) (2004).

References

1 J. H. Burroughes, D. D. C. Bradley, A. R. Brown, R. N. Marks, K. Mackay, R. H. Friend, P. L. Burns, and A. B. Holmes, *Nature* **347**, 539 (1990).

2 F. L. Zhang, M. Johansson, M. R. Andersson, J. C. Hummelen, and O. Inganas, *Synthetic Metals* **137**, 1401 (2003).

3 S. V. Frolov, M. Shkunov, A. Fujii, K. Yoshino, and Z. V. Vardeny, *Ieee Journal of Quantum Electronics* **36**, 2 (2000).

4 A. J. Heeger, *Solid State Communications* **107**, 673 (1998).

5 R. J. Visser, *Philips Journal of Research* **51**, 467 (1998).

6 B. J. de Gans, P. C. Duineveld, and U. S. Schubert, *Advanced Materials* **16**, 203 (2004).

7 M. S. Jang, S. Y. Song, H. K. Shim, T. Y. Zyung, S. D. Jung, and L. M. Do, *Synthetic Metals* **91**, 317 (1997).

8 M. Suzuki, T. Hatakeyama, S. Tokito, and F. Sato, *Ieee Journal of Selected Topics in Quantum Electronics* **10**, 115 (2004).

9 P. Y. Bruice, *Organic Chemistry* (Prentice Hall, New Jersey, 1995).

10 Prentice Hall Media Portfolio, (Prentice Hall, 2004).

11 W. P. Su, J. R. Schrieffer, and A. J. Heeger, *Physical Review B* **22**, 2099 (1980).

12 W. P. Su, J. R. Schrieffer, and A. J. Heeger, *Physical Review Letters* **42**, 1698 (1979).

13 B. Schweitzer and H. Bassler, *Synthetic Metals* **109**, 1 (2000).

14 M. Pope and C. E. Swenberg, *Electronic Processes in Organic Crystals and Polymers* (Oxford University Press, Oxford, 1999).

15 P. W. M. Blom, M. J. M. de Jong, and C. Liedenbaum, *Polymers for Advanced Technologies* **9**, 390 (1998).

16 J. Mort, *Electronic Properties of Polymers* (Wiley, New York, 1982).

17 V. Dyakonov and E. Frankevich, *Chemical Physics* **227**, 203 (1998).

18 M. A. Baldo, D. F. O'Brien, M. E. Thompson, and S. R. Forrest, *Physical Review B* **60**, 14422 (1999).

19 M. Wohlgenannt, K. Tandon, S. Mazumdar, S. Ramasesha, and Z. V. Vardeny, *Nature* **409**, 494 (2001).

20 C. Rothe, in *Department of Physics* (MSc Thesis, University of Durham, Durham, 2002).

21 Y. V. Romanovskii, A. Gerhard, B. Schweitzer, U. Scherf, R. I. Personov, and H. Bassler, *Physical Review Letters* **84**, 1027 (2000).

22 T. H. Forster, in *10th Spiers Memorial Lecture*, 1959), p. 7.

23 J. R. Lakowicz, *Principals of Fluorescence Spectroscopy* (Kluwer Academic, New York, 1999).

24 D. L. Dexter, *Journal of Chemical Physics* **21**, 836 (1953).

25 S. V. Novikov, D. H. Dunlap, V. M. Kenkre, P. E. Parris, and A. V. Vannikov, *Physical Review Letters* **81**, 4472 (1998).

26 H. Bassler, *Physica Status Solidi B-Basic Research* **175**, 15 (1993).

27 C. Rothe and A. P. Monkman, *Physical Review B* **68**, 075208 (2003).

28 D. Hertel, H. Bassler, R. Guentner, and U. Scherf, *Journal of Chemical Physics* **115**, 10007 (2001).

[29] R. Jakubiak, C. J. Collison, W. C. Wan, L. J. Rothberg, and B. R. Hsieh, *Journal of Physical Chemistry A* **103**, 2394 (1999).
[30] M. Yan, L. J. Rothberg, F. Papadimitrakopoulos, M. E. Galvin, and T. M. Miller, *Physical Review Letters* **73**, 744 (1994).
[31] S. Hintschich, C. Rothe, and A. P. Monkman, (submitted).
[32] E. J. W. List, R. Guentner, P. S. de Freitas, and U. Scherf, *Advanced Materials* **14**, 374 (2002).
[33] B. P. Straughan and S. Walker, *Spectroscopy* (Chapman and Hall, London, 1976).
[34] P. O'connor and J. Tauc, *Physical Review B* **25**, 2748 (1982).
[35] S. King, C. Rothe, and A. Monkman, *Journal of Chemical Physics*, (in press) (2004).
[36] D. M. Johansson, M. Theander, T. Granlund, O. Inganas, and M. R. Andersson, *Macromolecules* **34**, 1981 (2001).
[37] W. J. Feast and R. H. Friend, *Journal of Materials Science* **25**, 3796 (1990).
[38] J. H. Hsu and W. S. Fann, *Synthetic Metals* **101**, 214 (1999).
[39] M. Wohlgenannt, W. Graupner, R. Osterbacka, G. Leising, D. Comoretto, and Z. V. Vardeny, *Synthetic Metals* **101**, 267 (1999).
[40] B. Schweitzer, V. I. Arkhipov, U. Scherf, and H. Bassler, *Chemical Physics Letters* **313**, 57 (1999).
[41] V. Dyakonov, G. Rosler, M. Schwoerer, and E. L. Frankevich, *Physical Review B* **56**, 3852 (1997).
[42] A. P. Monkman, H. D. Burrows, M. D. Miguel, I. Hamblett, and S. Navaratnam, *Chemical Physics Letters* **307**, 303 (1999).
[43] R. D. Scurlock, B. J. Wang, P. R. Ogilby, J. R. Sheats, and R. L. Clough, *Journal of the American Chemical Society* **117**, 10194 (1995).
[44] M. Smoluchowski, *Zeitschrift fuer Physikalische Chemie* **92**, 129 (1917).
[45] B. Movaghar, B. Ries, and M. Grunewald, *Physical Review B* **34**, 5574 (1986).
[46] B. Ries and H. Bassler, *Journal of Molecular Electronics* **3**, 15 (1987).
[47] D. Beljonne, G. Pourtois, C. Silva, E. Hennebicq, L. M. Herz, R. H. Friend, G. D. Scholes, S. Setayesh, K. Mullen, and J. L. Bredas, *Proceedings of the National Academy of Sciences of the United States of America* **99**, 10982 (2002).
[48] A. P. Monkman, H. D. Burrows, I. Hamblett, S. Navarathnam, M. Svensson, and M. R. Andersson, *Journal of Chemical Physics* **115**, 9046 (2001).
[49] J. S. de Melo, *Journal of Chemical Physics* **111**, 5427 (1999).
[50] H. Meier, U. Stalmach, and H. Kolshorn, *Acta Polymerica* **48**, 379 (1997).
[51] D. A. Dos Santos, N. Beijonne, J. Cornil, and J. L. Bredas, *Synthetic Metals* **85**, 1025 (1997).
[52] K. Mullen and G. Wegner, *Electronic Materials: The Oligomer Approach* (Wiley-VCH, Weinheim, 1998).
[53] J. Rissler, *Chemical Physics Letters* **395**, 92 (2004).
[54] H. Meier, U. Stalmach, and H. Kolshorn.
[55] A. J. Heeger, S. Kivelson, J. R. Schrieffer, and W. P. Su, *Reviews of Modern Physics* **60**, 781 (1988).
[56] M. Bennati, A. Grupp, P. Bauerk, and M. Mehring, *Molecular Crystals and Liquid Crystals* **256**, 751 (1994).
[57] L. S. Swansson, J. Shinar, and K. Yoshino, *Physical Review Letters* **65**, 781 (1990).
[58] J. H. Park, H. C. Ko, J. H. Kim, and H. Lee, *Synthetic Metals* **144**, 193 (2004).

[59] A. van Dijken, J. Bastiaansen, N. M. M. Kiggen, B. M. W. Langeveld, C. Rothe, A. Monkman, I. Bach, P. Stossel, and K. Brunner, *Journal of the American Chemical Society* **126**, 7718 (2004).
[60] A. J. Cadby, P. A. Lane, H. Mellor, S. J. Martin, M. Grell, C. Giebeler, D. D. C. Bradley, M. Wohlgenannt, C. An, and Z. V. Vardeny, *Physical Review B* **62**, 15604 (2000).
[61] M. Ariu, D. G. Lidzey, and D. D. C. Bradley, *Synthetic Metals* **111**, 607 (2000).
[62] O. J. Korovyanko and Z. V. Vardeny, *Chemical Physics Letters* **356**, 361 (2002).
[63] U. Lemmer, S. Heun, R. F. Mahrt, U. Scherf, M. Hopmeier, U. Siegner, E. O. Gobel, K. Mullen, and H. Bassler, *Chemical Physics Letters* **240**, 373 (1995).
[64] M. A. Baldo, S. Lamansky, P. E. Burrows, M. E. Thompson, and S. R. Forrest, *Applied Physics Letters* **75**, 4 (1999).
[65] C. Y. Jiang, W. Yang, J. B. Peng, S. Xiao, and Y. Cao, *Advanced Materials* **16**, 537 (2004).
[66] D. F. O'Brien, C. Giebeler, R. B. Fletcher, A. J. Cadby, L. C. Palilis, D. G. Lidzey, P. A. Lane, D. D. C. Bradley, and W. Blau, *Synthetic Metals* **116**, 379 (2001).
[67] C. Adachi, M. A. Baldo, S. R. Forrest, S. Lamansky, M. E. Thompson, and R. C. Kwong, *Applied Physics Letters* **78**, 1622 (2001).
[68] C. L. Lee, K. B. Lee, and J. J. Kim, *Applied Physics Letters* **77**, 2280 (2000).
[69] R. A. Negres, X. Gong, J. C. Ostrowski, G. C. Bazan, D. Moses, and A. J. Heeger, *Physical Review B* **68**, art. no. (2003).
[70] X. Gong, J. C. Ostrowski, D. Moses, G. C. Bazan, and A. J. Heeger, *Advanced Functional Materials* **13**, 439 (2003).
[71] J. Kalinowski, W. Stampor, M. Cocchi, D. Virgili, V. Fattori, and P. Di Marco, *Chemical Physics* **297**, 39 (2004).
[72] C. Rothe, L. O. Palsson, and A. P. Monkman, *Chemical Physics* **285**, 95 (2002).
[73] A. B. Tamayo, B. D. Alleyene, P. I. Djurovivich, S. Lamansky, I. Tsyba, N. N. Ho, R. Ho, M. E. Bau, and M. E. Thompson, *Journal of the American Chemical Society* **125**, 7377 (2003).
[74] P. J. Hay, *Journal of Physical Chemistry A* **106**, 1634 (2002).
[75] K. Tang, L. L. Kuan, and I. Chen, *Chemical Physics Letters* **386**, 437 (2004).
[76] M. Sainsbury, *Aromatic Chemistry* (Oxford Science Publications, Oxford, 1992).
[77] R. J. Watts, K. A. King, K. Ichimura, and T. Kobayashi, *Journal of Physical Chemistry* **91**, 6104 (1987).
[78] J. Mort and G. Pfister, *Electronic Properties of Polymers* (John Wiley and Sons, New York, 1982).